

A MONOSTABLE MULTIVIBRATOR WITH THE TIMING PERIOD  
INDEPENDENT OF SUPPLY VOLTAGE.

by

Gordon K. Shipp

---

A Thesis Submitted to the Faculty of the  
DEPARTMENT OF ELECTRICAL ENGINEERING  
In Partial Fulfillment of the Requirements  
For the Degree of  
MASTER OF SCIENCE  
In the Graduate College  
THE UNIVERSITY OF ARIZONA

1961

# STATEMENT BY AUTHOR

This thesis has been submitted in partial fulfillment of requirements for an advanced degree at The University of Arizona and is deposited in The University Library to be made available to borrowers under rules of the Library.

Brief quotations from this thesis are allowable without special permission, provided that accurate acknowledgment of source is made. Requests for permission for extended quotation from or reproduction of this manuscript in whole or in part may be granted by the head of the major department or the Dean of the Graduate College when in their judgment the proposed use of the material is in the interests of scholarship. In all other instances, however, permission must be obtained from the author.

SIGNED: Gordon K. Shipp

## APPROVAL BY THESIS DIRECTOR

This thesis has been approved on the date shown below:

Paul G. Griffith  
PAUL G. GRIFFITH  
Associate Professor of Electrical Engineering

May 4, 1961  
Date

## ABSTRACT

### A MONOSTABLE MULTIVIBRATOR WITH THE TIMING PERIOD INDEPENDENT OF SUPPLY VOLTAGE

by

Gordon K. Shipp

This thesis presents an analysis of a vacuum-tube triode and a transistor monostable multivibrator. It is shown that the timing period of the monostable multivibrator is independent of the power supply voltage, thereby making it ideally suited wherever well-regulated supplies are not available.

Circuit models are developed that will approximate the behavior of the vacuum-tube triode and transistor. By the proper use of these linear circuit models, a nonlinear problem is solved by the method of linear circuit analysis.

The description of the operation of the multivibrators is presented concurrently with the analysis of the circuits. The design criteria, voltage waveforms, and performance characteristics evolve from this analysis. Mathematically, the timing period of these multivibrators is proven to be independent of the value of the supply voltage.

An experimental circuit is designed, constructed, and tested for both the vacuum-tube and transistor multivibrators. The measured results show excellent correlation with the values calculated from the mathematical formulas. For the vacuum-tube circuit, a change of 50% in the supply voltage caused only a 2.3% change in the timing period. Correspondingly, only a 0.51% variation was noted in the timing period of the transistor monostable multivibrator.

## ACKNOWLEDGMENTS

The author wishes to express his sincere appreciation to Dr. Paul G. Griffith for his constructive suggestions and criticisms during the course of this study and in the preparation of this manuscript.

Appreciation is also extended to Mr. Paul Welch of the Hughes Aircraft Company for his assistance and suggestions.

Sincere thanks are due to the staff of the Tucson Engineering Laboratory, Hughes Aircraft Company. This work was carried out while the writer was a member of the Technical Staff at the Tucson Engineering Laboratory and a holder of a Hughes M. S. Fellowship.

The writer gratefully acknowledges the assistance and understanding of his wife, Wyona, throughout the conduct of the study and in preparation of this thesis.

## TABLE OF CONTENTS

	Page
Statement By Author	i
Abstract	ii
Acknowledgment	iii
Table of Contents	iv
List of Tables	vi
List of Illustrations	vii
 CHAPTER	
1. INTRODUCTION	1
1.1 Background	1
1.2 Statement of the Problem	2
1.3 Scope	4
2. VACUUM-TUBE TRIODE AND TRANSISTOR CIRCUIT MODELS	5
2.1 Introduction	5
2.2 Vacuum-Tube Triode Circuit Models	6
2.2.1 Region I Operation	6
2.2.2 Region II Operation	8
2.2.3 Region III Operation	10
2.3 Transistor Circuit Models	12
2.3.1 Region I Operation	14
2.3.2 Region II Operation	14
2.3.3 Region III Operation	18
3. ANALYSIS OF THE VACUUM-TUBE MONOSTABLE MULTIVIBRATOR	20
3.1 Introduction	20
3.2 Stable State Operation	20
3.3 Quasi-Stable State Operation	25
3.4 Calculation of the Timing Period	30
3.5 Triggering of the Monostable Multivibrator	35

## TABLE OF CONTENTS (continued)

	Page
4. ANALYSIS OF THE TRANSISTOR MONOSTABLE MULTIVIBRATOR	39
4.1 Introduction	39
4.2 Stable State Operation	39
4.3 Quasi-Stable State Operation	43
4.4 Transistor Circuit Triggering	46
5. EXPERIMENTAL TEST RESULTS	49
5.1 Test Procedure	49
5.2 Vacuum-Tube Experimental Results	49
5.3 Transistor Experimental Results	56
6. CONCLUSIONS	61
6.1 Performance Evaluation	61
6.2 Recommendations for further study	61
APPENDIX	
A. The Derivation of the Timing Period for the Case Where $T_1$ is in Clamp	63
B. The Derivation of the Timing Period for the Transistor Circuit	65
BIBLIOGRAPHY	67

# LIST OF TABLES

<u>TABLE</u>		Page
I	Stable State Voltage Equations	24
II	Quasi-Stable State Voltage Equations	27
III	Transistor Stable State Voltage Equations	43
IV	Transistor Quasi-Stable State Voltage Equations	45
V	Experimental Results for the Vacuum-Tube Monostable Multivibrator Circuit -- Measured and Calculated Voltage Values	54
VI	Experimental Results for the Vacuum-Tube Monostable Multivibrator Circuit -- Per Cent Change in T versus Per Cent Change in $E_{bb}$	56
VII	Experimental Results for the Transistor Monostable Multivibrator Circuit -- Measured and Calculated Voltage Values	58
VIII	Experimental Results for the Transistor Monostable Multivibrator Circuit -- Per Cent Change in T versus Per Cent Change in $E_{cc}$	60

## LIST OF ILLUSTRATIONS

<u>FIGURE</u>	<u>Page</u>
2.1 Circuit Utilized for Development of the Vacuum-Tube Triode Models	7
2.2 Typical Plate Characteristic Curves of a Vacuum-Tube Triode	7
2.3 Idealized Characteristic Curves for Operation in Region II	9
2.4 Equivalent Circuit for Operation in Region II and III	9
2.5 Vacuum-Tube Triode Circuit Models	11
2.6 Circuit Utilized for Development of the Transistor Models	13
2.7 Typical Transistor Characteristic Curves	15
2.8 Idealized Collector Characteristics for Operation in Region II	17
2.9 Base Parameters for Operation in Region II	17
2.10 Transistor Circuit Models	19
3.1 Vacuum-Tube Monostable Multivibrator	21
3.2 Equivalent Circuit for Operation in the Stable State	23
3.3 Equivalent Circuit for Operation in the Quasi-Stable State	26
3.4 Idealized Voltage Waveforms of the Vacuum-Tube Monostable Multivibrator	29
3.5 Effective Plate Supply Voltage and Load Resistance of Tube $T_1$ for Operation in Region II	31
3.6 Graphical Method for Determining the Operating Point of $T_1$ for Operation in the Quasi-Stable State	31
3.7 Simplified Equivalent Circuit for Operation in the Quasi-Stable State	33

## LIST OF ILLUSTRATIONS (continued)

<u>FIGURE</u>	<u>Page</u>
3.8 Calculation of the time constant for Operation in the Quasi-Stable State.	33
3.9 Generalized Exponential Waveform	37
3.10 Recommended Method for Triggering the Vacuum-Tube Monostable Multivibrator	37
4.1 Transistor Monostable Multivibrator	40
4.2 Equivalent circuit for Operation in the Stable State	41
4.3 Equivalent Circuit for Operation in the Quasi-Stable State	44
4.4 Idealized Voltage Waveforms of the Transistor Monostable Multivibrator	47
5.1 Block Diagram of the Experimental Setup	50
5.2 Experimental Vacuum-Tube Monostable Multivibrator	51
5.3 Characteristic Curves for a 12AT7 Vacuum-Tube Triode	53
5.4 Output Waveform of the Vacuum-Tube Monostable Multivibrator for different Values of Supply Voltage	55
5.5 Experimental Transistor Monostable Multivibrator	57
5.6 Output Waveform of the Transistor Monostable Multivibrator for Different Values of Supply Voltage	59

## CHAPTER 1

### INTRODUCTION

#### 1.1 BACKGROUND

The multivibrator is a versatile type of circuit that finds widespread application in pulse and digital circuits. In its most common form, the multivibrator incorporates two stages of amplification with feedback from the output of one stage to the input of the other stage. Any disturbance or signal at an input will be amplified through the two stages, which are effectively in cascade, and then will reappear at the original input with such a polarity as to aid the initial disturbance. This action constitutes the regenerative property of the circuit, the property that can be shown to cause the circuit to drive itself into one or the other of its two states of operation; i.e., stable or quasi-stable. The circuit action is stable if it remains permanently in the same operating condition until acted upon by an external trigger pulse. In contrast, the circuit action is quasi-stable if it remains only temporarily in a particular mode of operation. At the end of the quasi-stable state, the circuit will automatically regenerate to its other state of operation, which may be either stable or quasi-stable.

The existence of these two states allows the multivibrator to be divided into three principal sub-classes: the bistable, astable,

and monostable. The bistable multivibrator can remain indefinitely in either of its stable states when free of external influences. In contrast, the astable multivibrator has two quasi-stable states and oscillates between the two states with a temporary period of time expended in each state. The monostable multivibrator is a combination of these two circuits, having one stable and one quasi-stable state. The monostable multivibrator will remain permanently in its stable state until placed in the quasi-stable state by the application of a trigger pulse. After a predetermined length of time, the circuit will automatically regenerate back to its stable mode of operation. The circuit will then provide an output pulse of a particular width for each trigger input. The width of this output pulse is essentially independent of the trigger signal and is determined, in most cases, by an RC time constant. The monostable multivibrator will be the subject under discussion in this thesis.

## 1.2 STATEMENT OF THE PROBLEM

In pulse and digital circuits, there exists a definite need for pulses of a particular width. A few of these circuits are transmission gates, time delays, voltage comparators, coincidence comparators, and sawtooth generators. It is extremely important that the width of the pulse, which is provided by the monostable multivibrator, does not change with repeated cycling. It can be shown, however, that the

plate-coupled and cathode-coupled monostable multivibrators are very sensitive to changes in the supply voltage.\* In fact, it is not uncommon for a 10% change in the supply voltage to cause a 5 to 10% change in the pulse width.<sup>1</sup> This is not a serious problem where well-regulated power supplies are available. However, there are many instances where it is not feasible to have a well-regulated supply due to its excessive bulk and cost. In many cases, the supply voltage will be provided by a source of power which has an output voltage that is constantly changing as time progresses. For reliable operation, the circuit behavior must be insensitive to this change in supply voltage.

It will be the aim of this thesis to analyze and test a monostable multivibrator that exhibits excellent independence of changes in the supply voltage. In contrast to the popular plate-coupled monostable multivibrator, this circuit also requires only a single power supply. It is true that the cathode-coupled multivibrator requires only a single power supply, but this circuit has the disadvantage that it is very sensitive to changes that may occur in the supply voltage.

---

\*This argument also applies to the transistor monostable multivibrators.

<sup>1</sup>J. Millman and H. Taub, Pulse and Digital Circuits, McGraw-Hill Book Company, Inc., New York, 1956, pg 194

### 1.3 SCOPE

Since the circuits to be analyzed operate in a nonlinear fashion, the circuit models that will be used to approximate the behavior of the vacuum-tube triode and transistor will be developed in Chapter 2. By the proper use of these circuit models, this nonlinear problem will be solved by the methods of linear circuit analysis. Since the circuits will be designed around ten per cent components, it is not necessary to insist on a precision analysis. The circuit can, of course, be adjusted to better than one per cent performance since the first order analysis reveals the elements that govern the circuit behavior.

The vacuum-tube monostable multivibrator will be analyzed in Chapter 3 with the analysis of its transistor counterpart to follow in Chapter 4. The design criteria, voltage waveforms, and performance characteristics of the circuits will evolve from this analysis.

In order to substantiate the validity of the theoretical analysis, experimental circuits are designed, constructed, and tested for both the vacuum-tube and transistor circuits. The circuits are tested to demonstrate the independence of the pulse width to changes in the supply voltage. The comparison between the calculated and measured values will be given in Chapter 5. A summary of the results and recommendations for further study will be given in Chapter 6.

## CHAPTER 2

### VACUUM-TUBE TRIODE AND TRANSISTOR CIRCUIT MODELS

#### 2.1 INTRODUCTION

The circuit models that will be used to represent the vacuum-tube triode and transistor must be developed in the beginning in order to simplify the operating principles and to avoid unnecessary duplications. Since an exact analysis of the circuits to be considered is not possible, these models will be used to approximate the properties of the nonlinear device. By the proper use of these linear circuit models, a nonlinear problem can be solved by the methods of linear circuit analysis. Even though these models will not be exact, it will be shown later in the experimental results that the approximations are sufficiently accurate for engineering purposes.

For these devices, it is possible to define three distinct regions of operation. These regions will be referred to as Regions I, II, and III and are briefly defined as follows:

1. Region I is that region of operation where the device is said to be cut off; that is, no current is allowed to flow in the output circuit.
2. Region II is normally referred to as the active or linear region of operation and is where the device is usually utilized for linear amplification.

3. Region III is characterized by the action known as clamping. Clamping is a property where the output current is not influenced by the input circuit.

These three regions of operation will be considered separately, and the circuit models will be developed for each region.

## 2.2 VACUUM-TUBE TRIODE CIRCUIT MODELS

The circuit to be considered is shown in Fig. 2.1 where the appropriate current and voltages have been defined. By the overlay of a load line on the plate characteristic curves of the triode, it is possible to perform a graphical analysis of the circuit. The load line, as determined from the circuit, can be expressed by the equation

$$E_b = E_{bb} - I_b R_L \quad 2.1$$

The plate characteristic curves represent a graphical plot of the relationship that exists among the plate current, plate voltage, and the grid voltage. An example of the solution for the plate current and voltage is shown in Fig. 2.2 using the assumed values of 200 volts for  $E_{bb}$ , 25 kilohms for  $R_L$ , and -4 volts for  $e_g$ . By the proper selection of  $e_g$ , the tube can be made to operate in any one of the three regions shown in Fig. 2.2.

### 2.2.1 REGION I OPERATION

When the grid voltage  $e_g$  becomes sufficiently negative to cause plate current to cease, the tube enters the cut off region. Since no current flows through  $R_L$ , the voltage at the plate of the

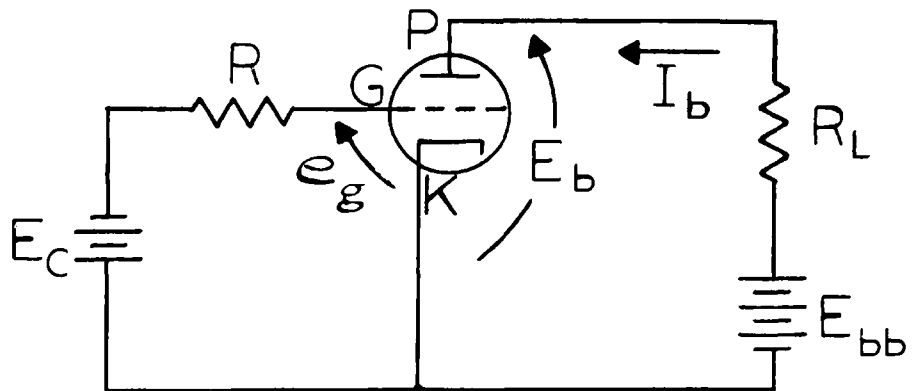


FIGURE 2.1

CIRCUIT UTILIZED FOR DEVELOPMENT OF THE VACUUM-TUBE TRIODE MODELS

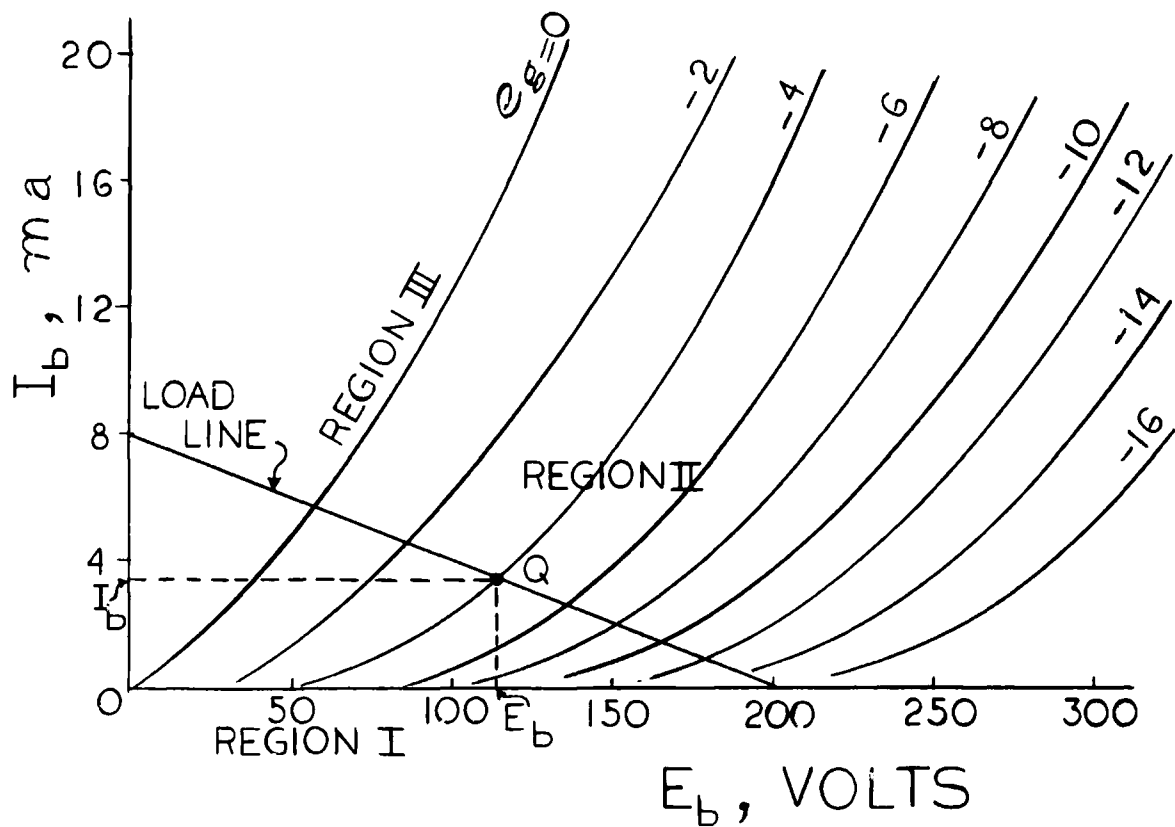


FIGURE 2.2

TYPICAL PLATE CHARACTERISTIC CURVES OF A VACUUM-TUBE TRIODE

tube becomes equal to  $E_{bb}$ . The operation in Region I, therefore, yields a very simple model as the action of the tube is approximated by an open circuit as shown in Fig. 2.5 (a).

### 2.2.2 REGION II OPERATION

Since there is no ac signal input to the circuit of Fig. 2.1, the operation of the tube in Region II is held to a single point which is located on the load line. The tube parameters  $\mu$  and  $r_p$  are indicative of the spacing and slope, respectively, of the characteristic curves. Since the operating point is fixed, once the value for  $e_g$  is known, the tube parameters are considered to be constants and can be calculated at the point of interest. These values are given by:

$$\mu = - \frac{\Delta E_b}{\Delta E_c} \Big/ I_b = \text{Constant} \quad 2.2$$

$$r_p = \frac{\Delta E_b}{\Delta I_b} \Big/ E_c = \text{Constant} \quad 2.3$$

The assumption that the curves are linear, with the above spacing and slope, will introduce no error in the calculation of  $I_b$  and  $E_b$  if the point of operation is not changed. Extrapolation of the  $e_g$  curves around the operating point will yield the idealized curves shown in Fig. 2.3, where the voltage  $E_0$  is an intercept adjuster that compensates for the shift in the  $e_g = 0$  curve.

The voltage at the intercept of an  $e_g$  curve is given by:

$$E = E_0 - \mu e_g \quad 2.4$$

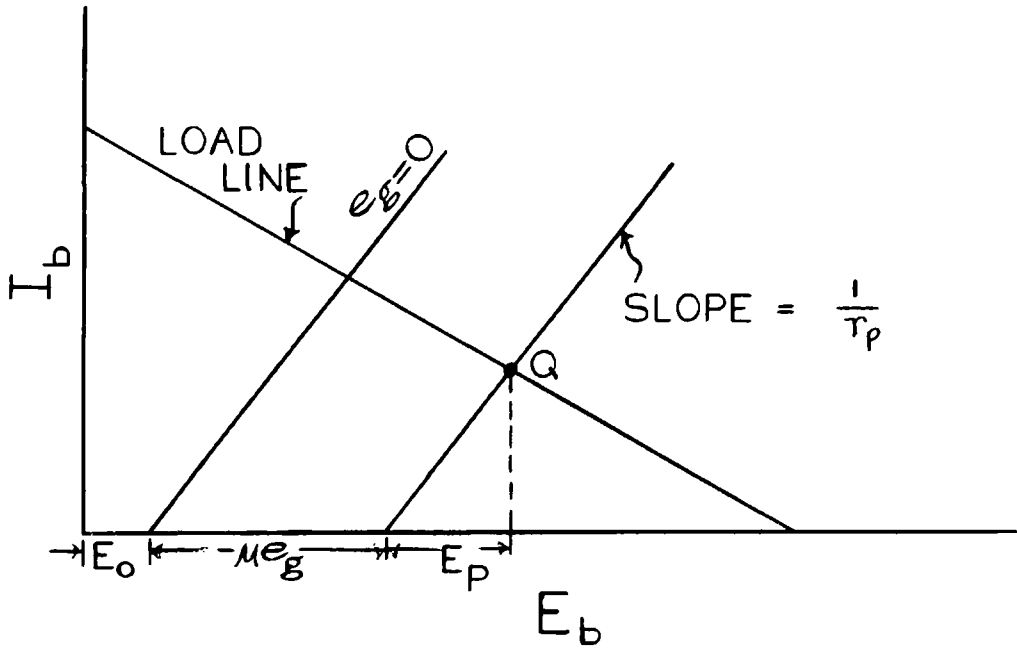
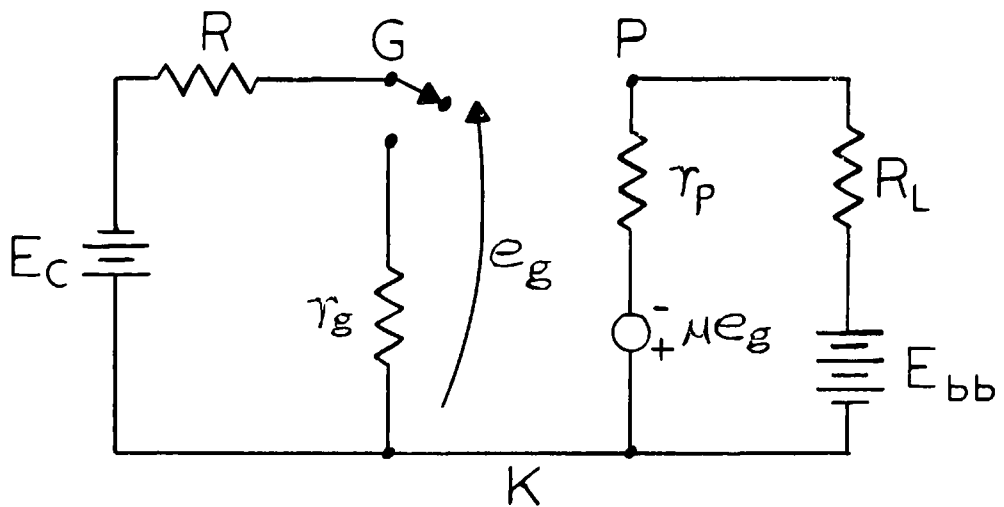


FIGURE 2.3

IDEALIZED CHARACTERISTIC CURVES FOR OPERATION IN REGION II



SWITCH IS SHOWN IN POSITION FOR OPERATION IN REGION II

FIGURE 2.4

EQUIVALENT CIRCUIT FOR OPERATION IN REGION II AND III

This voltage is not the total voltage across the tube, but has in addition the voltage specified as  $E_p$ . The voltage  $E_p$  is due to the finite slope of the  $e_g$  curve and has a value represented by:

$$E_p = I_b r_p \quad 2.5$$

The voltage across the tube can be defined as the sum of these two equations and has a value of

$$E_b = E_o - \mu E_c + I_b r_p \quad 2.6$$

For this study, the voltage  $E_o$  will be omitted from this equation since it is assumed to be negligible when compared with the magnitude of the other voltages.

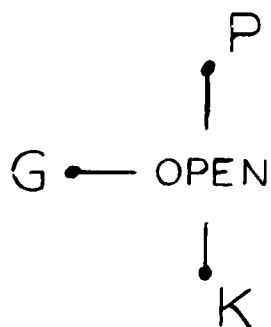
On the basis of the above assumptions, a simplified expression for the cut-off voltage,  $E_{co}$ , will evolve from the solution of  $E_q$  2.4. The value of this cut-off voltage is given by:

$$E_{co} = - \frac{E_{bb}}{\mu} \quad 2.7$$

Replacing the tube with its equivalent voltage yields the circuit of Fig. 2.4. The switch is shown in the proper position for operation in Region II. When  $e_g$  reaches a value of zero, the switch will reverse its position. The circuit model that replaces the tube during Region II operation is depicted in Fig. 2.5 (b).

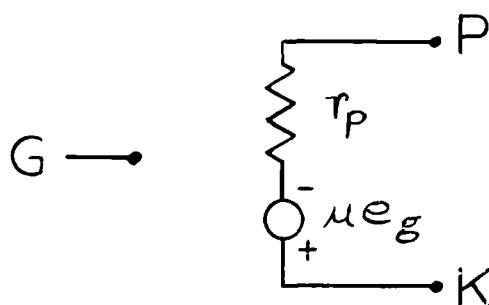
### 2.2.3 REGION III OPERATION

In Region III the tube is in saturation due to the grid-circuit clamping, thereby drawing its maximum plate current. In order to have



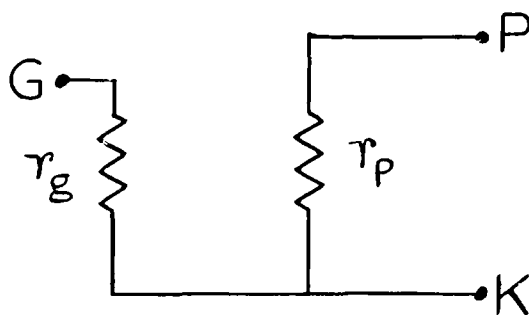
(a)

REGION I



(b)

REGION II



(c)

REGION III

FIGURE 2.5

VACUUM-TUBE TRIODE CIRCUIT MODELS

a better understanding of the action known as clamping, let us refer to Fig. 2.4. Whenever  $e_g$  becomes zero or positive, the switch reverses position and places  $r_g$  in the input circuit of the tube. The grid voltage  $e_g$  is then equal to

$$e_g = \frac{r_g E_c}{R + r_g} \approx 0 \quad 2.8$$

where  $r_g$  is the effective grid-to-cathode resistor for  $e_g \geq 0$ .

For this study, the value of  $R$  is selected to be much larger than  $r_g$ , thereby causing  $e_g$  to be essentially "clamped" to zero.

Since  $e_g$  has a value of approximately zero, the circuit model for Region III operation is shown in Fig. 2.5 (c). It should be remembered that the value for  $r_p$  is calculated at the operating point of the tube which, in this case, is at the intersection of the load line and the  $e_g = 0$  curve.

### 2.3 TRANSISTOR CIRCUIT MODELS

The circuit models for the transistor will now be developed from the circuit shown in Fig. 2.6. A p-n-p junction transistor will be chosen for this discussion since this type is also employed in the experimental work. The use of an n-p-n type would yield similar results. The voltage and current definitions are as shown in Fig. 2.6. By the overlay of a load line on the collector characteristic curves of the transistor, it is possible to perform a graphical analysis of the circuit. The load line, as determined from the circuit, is defined by the equation

$$E_c = E_{cc} - I_c R_L \quad 2.9$$

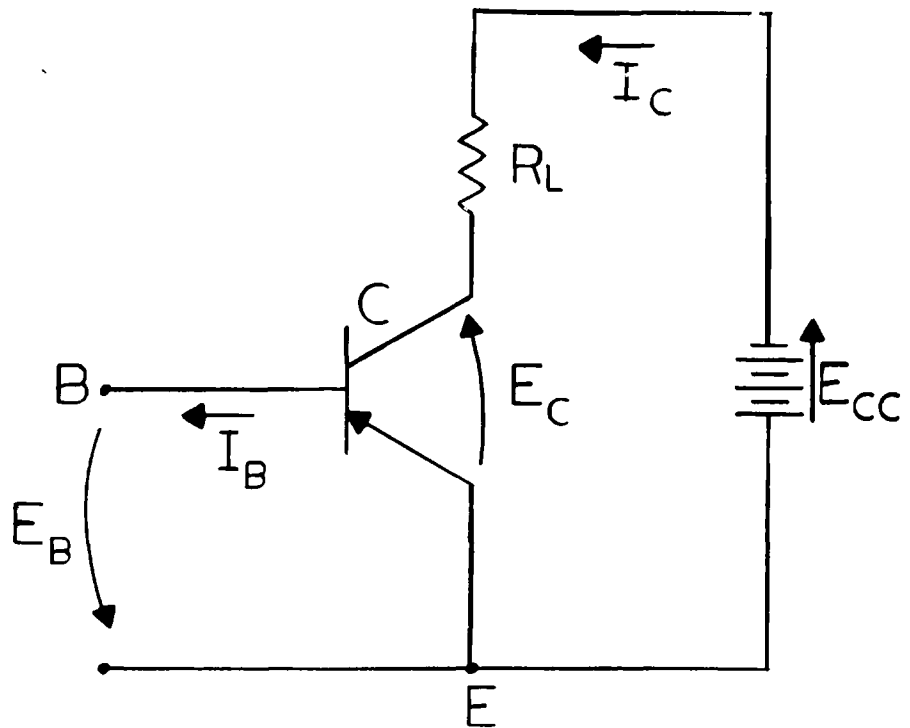


FIGURE 2.6

CIRCUIT UTILIZED FOR DEVELOPMENT OF THE TRANSISTOR MODELS

The collector characteristic curves represent a graphical plot of the relationship that exists among the collector current, collector voltage, and base current. An example of the solution for the collector current and voltage is shown in Fig. 2.7 (a) using the assumed values of -10 volts for  $E_{cc}$ , 5 kilohms for  $R_L$ , and  $20\mu a$  for  $I_B$ .

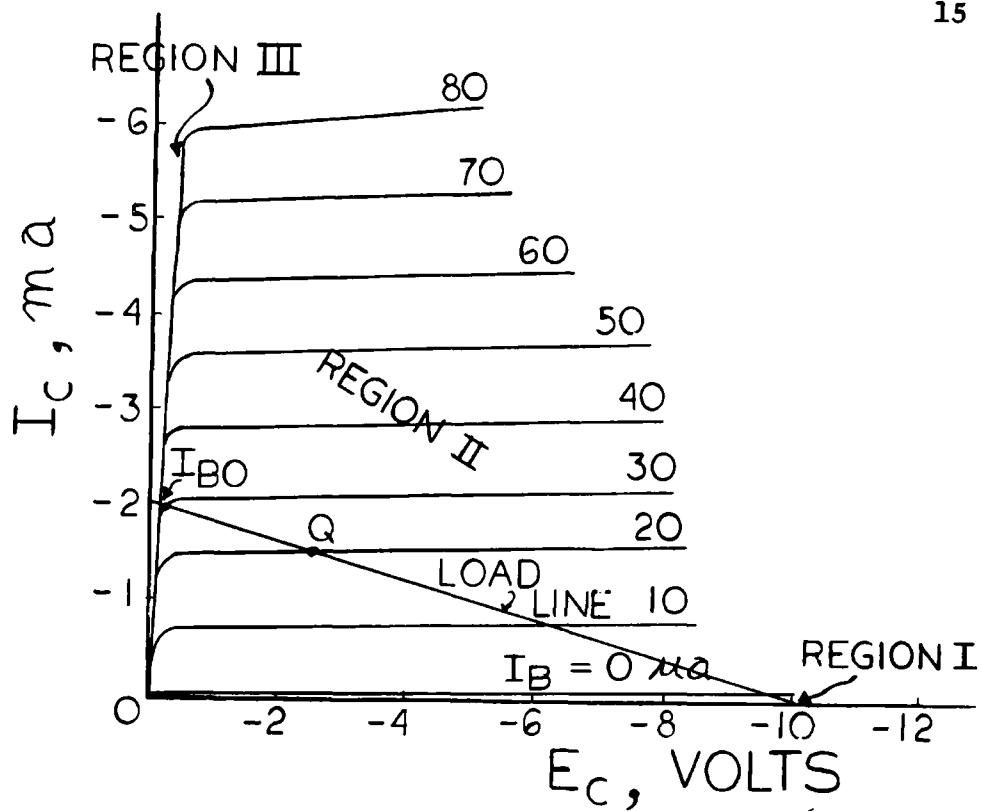
The curves shown in Fig. 2.7 (b) give the relationship that exists among the base current, base voltage, and collector voltage. These curves define the input circuit of the transistor and correspond to the grid characteristics of the triode when grid voltage is positive and grid current flows. By the proper selection of  $I_B$ , the transistor can be made to operate in any one of the three regions shown in Fig. 2.7 (a).

### 2.3.1 REGION I OPERATION

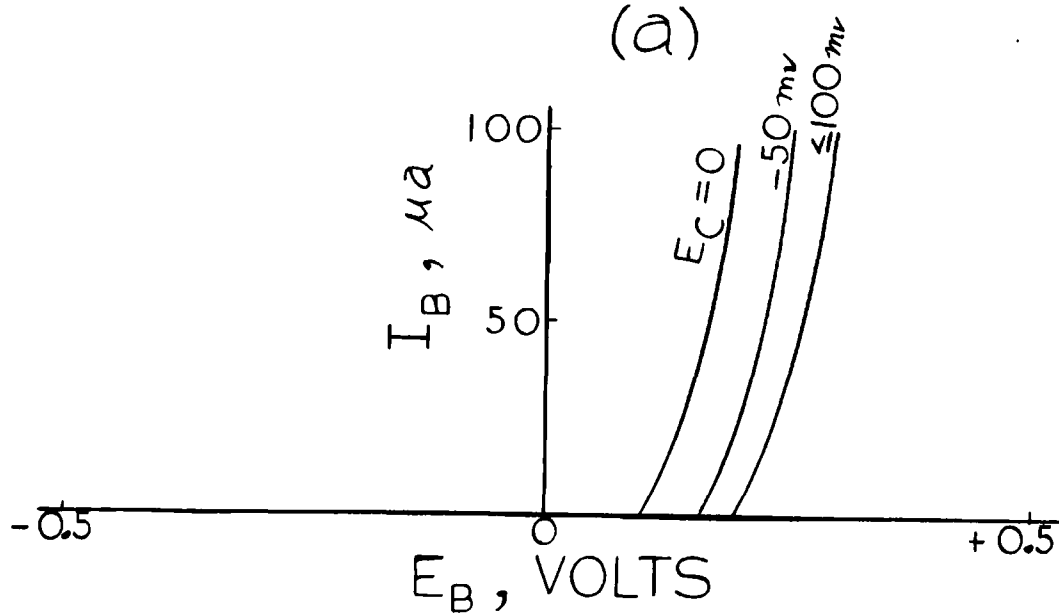
When the base current is reduced to zero, the transistor enters the cut-off region. For this study, the small residual current that does flow in the circuit is of such insignificance that this current can be neglected. Since no current flows through  $R_L$ , the collector voltage drops to a value equal to  $E_{cc}$ . For the operation in Region I, the input (base) and output (collector) circuits are approximated by open circuits as shown in Fig. 2.10 (a).

### 2.3.2 REGION II OPERATION

Reasoning similar to that of Section 2.2.2 indicates that the operating point of the transistor will be held to a single point located on the load line. The transistor parameters,  $\beta$  and  $r_c$ , are



(a)



(b)

FIGURE 2.7

TYPICAL TRANSISTOR CHARACTERISTIC CURVES  
 a) OUTPUT CHARACTERISTICS  
 b) INPUT CHARACTERISTICS

indicative of the spacing and slope, respectively, of the collector characteristic curves. Since the operating point is fixed, once the value for  $I_B$  is known, the transistor parameters are considered to be constants and are calculated at the point of interest. These values are given by:

$$\beta = \frac{\Delta I_c}{\Delta I_B} \Big/ E_c = \text{Constant} \quad 2.10$$

$$r_c = \frac{\Delta E_c}{\Delta I_c} \Big/ I_B = \text{Constant} \quad 2.11$$

The assumption that the curves are linear, with the above spacing and slope, will introduce no error in the calculation of  $E_c$  and  $I_c$  if the point of operation is not changed. The  $I_B$  curves of interest now appear as shown in Fig. 2.8. The current  $I_0$  is an intercept adjuster necessary to translate the family of current-voltage lines so that they coincide with the actual curves in the area of interest. The value of this current may be positive or negative and will be determined by the interception of the  $I_B = 0$  curve as shown in Fig. 2.8.

The current at the intercept of an  $I_B$  curve is given by:

$$I_c = I_0 + \beta I_B \quad 2.12$$

It is assumed that this is the total current since the curves are almost horizontal. For the input circuit model, reference is made to the input characteristic curves of Fig. 2.9. Since the operation of the base is in the region where  $E_c$  is larger than 0.1 volt, see Fig. 2.7 (b), the input circuit is replaced by a battery and a resistor

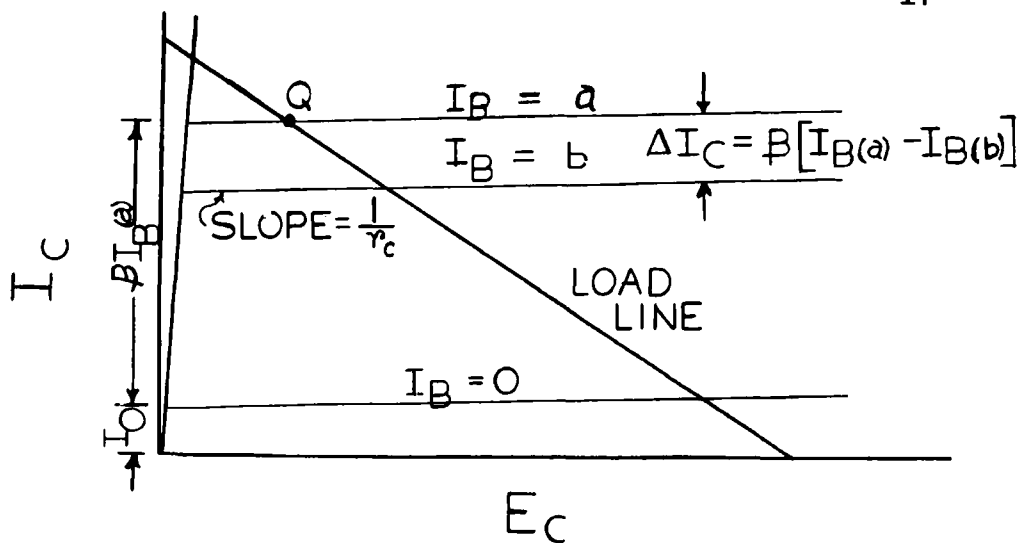


FIGURE 2.8

IDEALIZED COLLECTOR CHARACTERISTICS FOR OPERATION IN REGION II

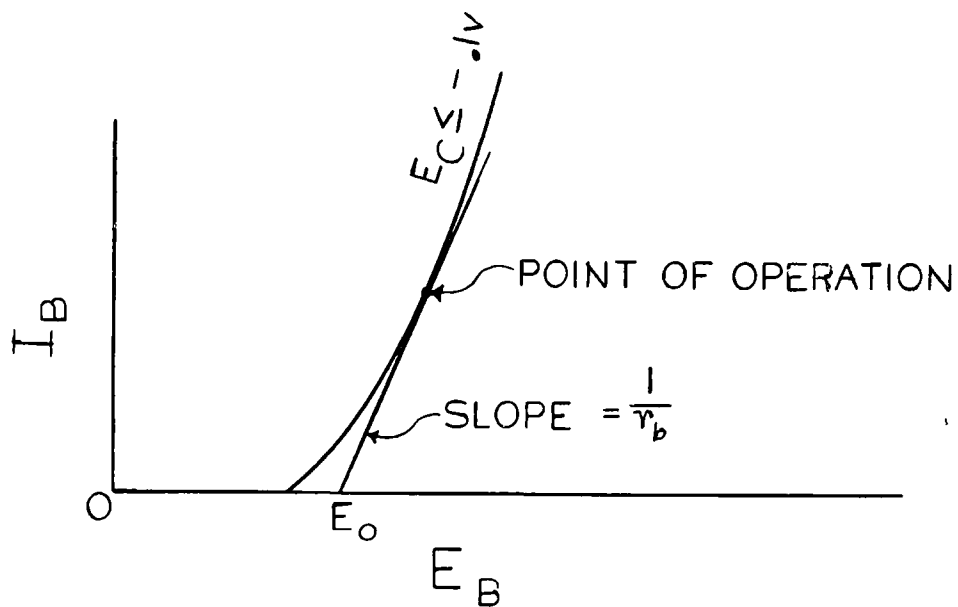


FIGURE 2.9

BASE PARAMETERS FOR OPERATION IN REGION II

which are calculated as shown in Fig. 2.9.

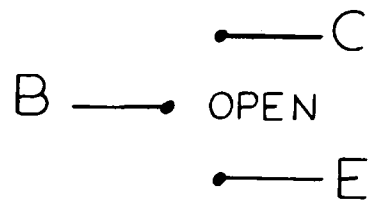
The input and output circuit models for the transistor during operation in Region II are shown in Fig. 2.10 (b).

### 2.3.3 REGION III OPERATION

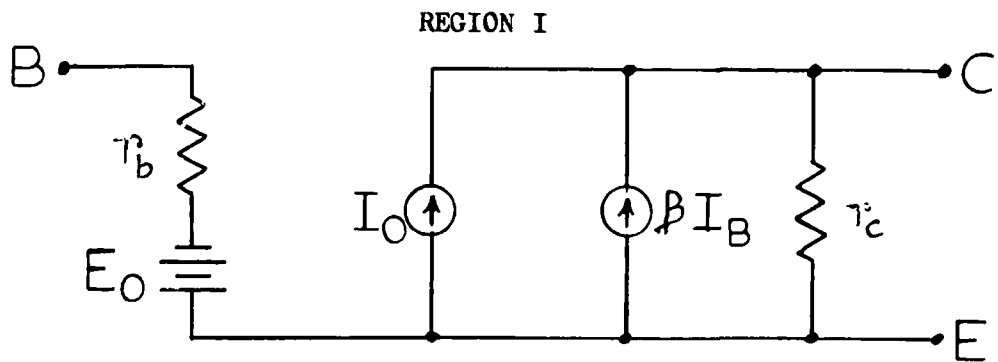
In this saturation region, the collector behaves like the anode of a simple diode with a low internal resistance, in the vicinity of 20 ohms for the transistors to be employed in this thesis. This resistance can be neglected when compared with  $R_L$  and the model then becomes a short circuit.

The development of the input model for Region III is identical to that of Region II. Its operation has now shifted, however, to the  $E_c = 0$  curve of Fig. 2.7 (b) and the values for  $r_b$  and  $E_o$  may be neglected.

The circuit model for the input and output of the transistor during operation in Region III is given in Fig. 2.10 (c).

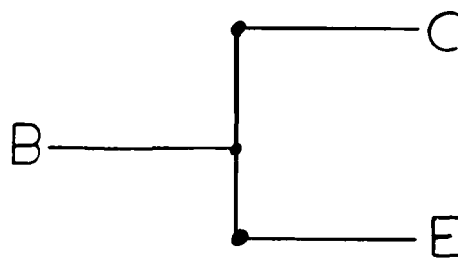


(a)



(b)

REGION II



(c)

REGION III

FIGURE 2.10

TRANSISTOR CIRCUIT MODELS

## CHAPTER 3

### ANALYSIS OF THE VACUUM-TUBE MONOSTABLE MULTIVIBRATOR

#### 3.1 INTRODUCTION

A monostable multivibrator whose timing period is independent of the power supply will be analyzed in this chapter. The description of the operation of this multivibrator will be divided into two parts, corresponding to the two states attributable to monostable action. The stable state will be considered first with the operation of the quasi-stable state to follow. The design criteria, voltage waveforms, and performance characteristics will evolve from this analysis.

The circuit under consideration is shown in Fig. 3.1 where the appropriate voltages and currents have been defined. It will be shown that the timing period of this circuit is independent of the supply voltage. In Chapter 5, experimental results will be given to substantiate the theoretical results of this chapter.

#### 3.2 STABLE STATE OPERATION

In order to assure reliable operation of the monostable multivibrator, it is necessary to have tube  $T_1$  cut off and tube  $T_2$  clamped during the stable state. The grid of  $T_2$  is connected, by the resistor  $R_1$ , to the positive voltage existing at the cathode of  $T_1$  which places  $T_2$  in a clamped condition ( $e_g \cong 0$ ). Since the values for the resistors  $R_1$  and  $R_2$  are selected to be much larger than  $R_{L2}$ , it is assumed that

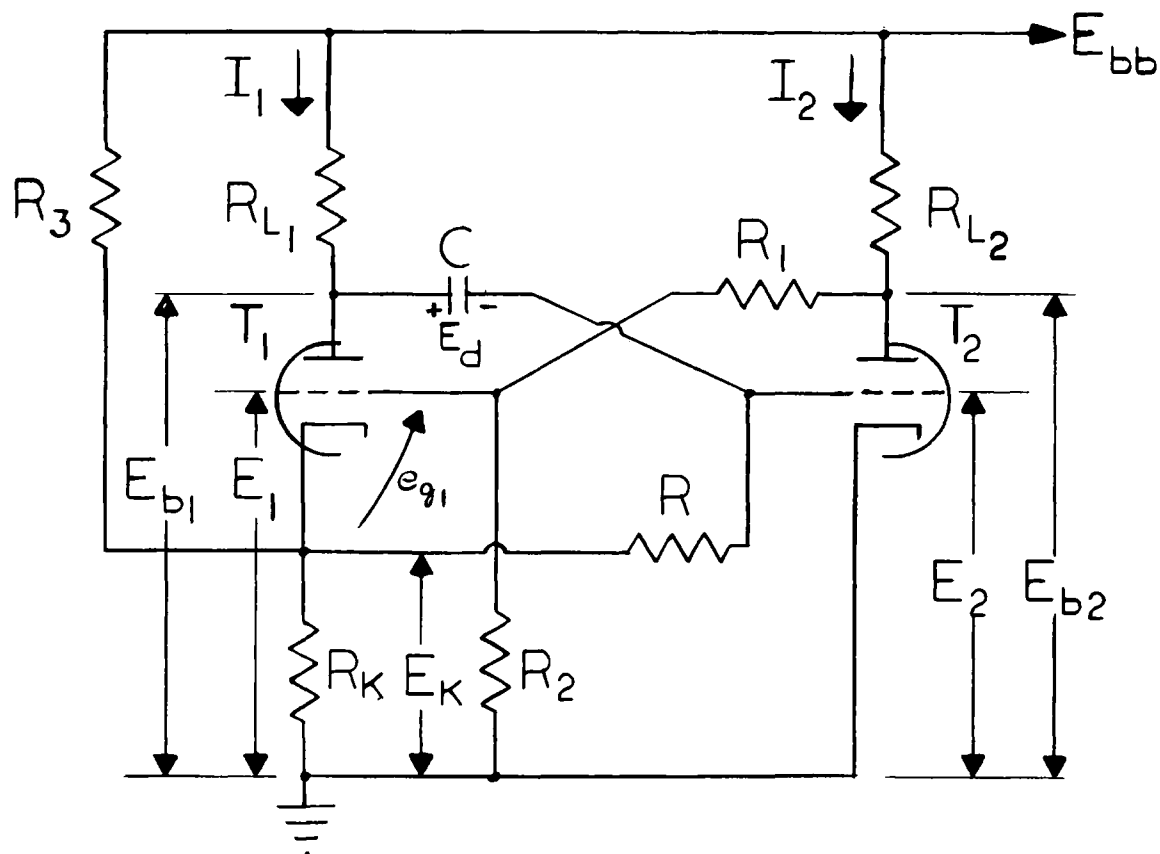


FIGURE 3.1

VACUUM-TUBE MONOSTABLE MULTIVIBRATOR

the current  $I_2$  flows entirely through the tube. The value of  $I_2$  is found graphically from the intersection of the load line and the  $e_g = 0$  curve.

By the proper selection of  $R_3$  and  $R_K$ , tube  $T_1$  is held in the cut-off condition. With  $T_1$  cut off and  $T_2$  in clamp, the circuit reduces to that of Fig. 3.2 where the tubes have been replaced by their circuit models.

The voltage  $E$  and resistor  $R_K'$  are products of the application of Thevenin's Theorem to the  $E_{bb}$ ,  $R_3$ , and  $R_K$  network and have values given by:

$$E = \frac{R_K E_{bb}}{R_K + R_3} \quad 3.1$$

$$R_K' = \frac{R_3 R_K}{R_3 + R_K} \quad 3.2$$

The voltages that result from operation in this state are given in Table I where

$$R \gg R_K' \quad 3.3$$

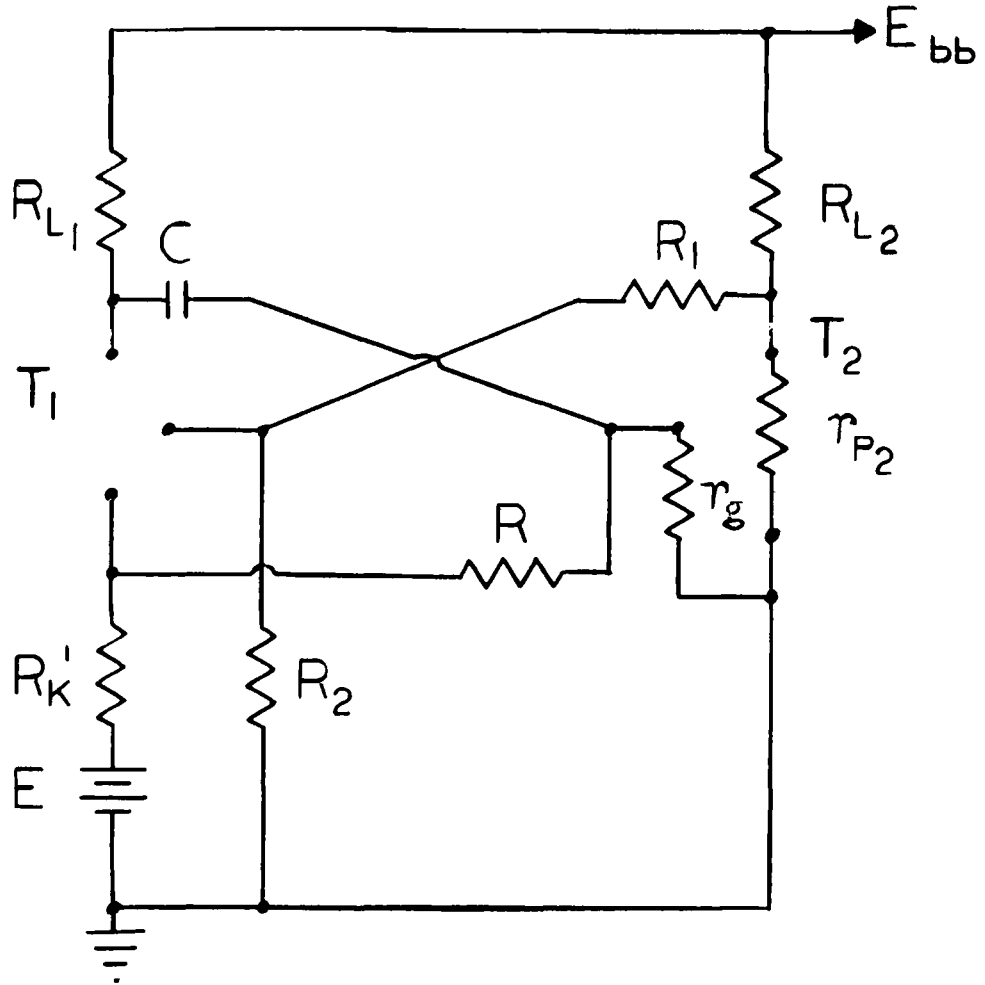


FIGURE 3.2

EQUIVALENT CIRCUIT FOR OPERATION IN THE STABLE STATE

TABLE I

## STABLE-STATE VOLTAGE EQUATIONS

VOLTAGE	VALUE
$E_{b1}$	$E_{bb}$
$E_{b2}$	$E_{bb} - I_2 R_{L2}$
$E_1$	$\frac{R_2}{R_1 + R_2} E_{b2}$
$E_2$	0
$E_K$	E
$e_{g1}$	$E_1 - E_K$
$E_d$	$E_{bb}$

The requirement that  $T_1$  be in a cut-off condition specifies that

$$E > E_1 - E_{col} \quad 3.4$$

where  $E_{col}$  is the cut-off voltage of  $T_1$  corresponding to an effective plate voltage of  $E_{bb} - E$ . Equation 3.4 will be satisfied over the expected range of  $E_{bb}$  if the proper values are selected for  $R_3$  and  $R_K$ . Factors to be considered in this selection include: the current drain from the power supply must be kept small, reasonable values for  $R_3$  and  $R_K$  must be used, and Eqs. 3.1 and 3.4 must be satisfied.

These conditions will prevail until the application of an external trigger causes a transition from the stable state to the quasi-stable state.

### 3.3 QUASI-STABLE STATE OPERATION

Let us reserve the discussion on triggering for a later section and assume that a transition has placed the circuit in the quasi-stable state of operation. The action during the transition drives  $T_2$  into cut off and  $T_1$  into operation in either the active region or the saturation region.\* In either case, a current  $I_1$  now flows in  $T_1$  and  $E_{b1}$  will drop by an amount equal to  $I_1 R_{L1}$ , with the same voltage change appearing at the grid of  $T_2$  due to the capacitive coupling between these two points.

The circuit at this instant appears as shown in Fig. 3.3 and calculation of the voltages, as defined in Fig. 3.1, yields the data given in Table II. The voltage  $E_1'$  will have a value of

$$E_1' = E_K \quad 3.5$$

or

$$E_1' = \frac{R_2}{R_1 + R_2} E_{bb} \quad 3.6$$

depending on the region of operation of  $T_1$ . Equation 3.5 applies when  $T_1$  is in the clamped condition and Eq. 3.6 applies when  $T_1$  is operating

---

\*Both of these regions of operation will be considered when the equation for the timing period is developed.

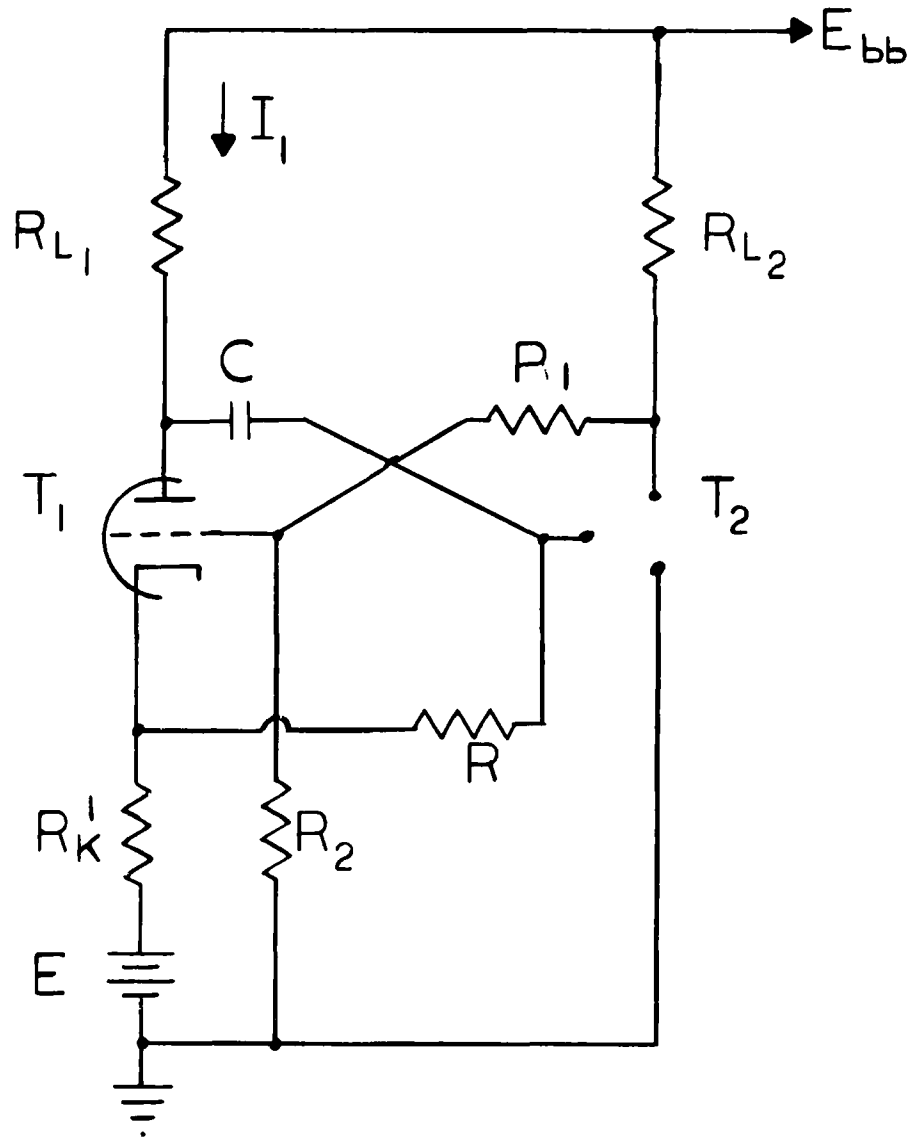


FIGURE 3.3

EQUIVALENT CIRCUIT FOR OPERATION IN THE QUASI-STABLE STATE

within its linear region. These two cases will be individually considered when the current  $I_1$  is calculated.

TABLE II

## QUASI-STABLE STATE VOLTAGE EQUATIONS

VOLTAGE	VALUE
$E_{b1}$	$E_{bb} - I_1 R_{L1}$
$E_{b2}$	$E_{bb}$
$E_K$	$E + I_1 R_K$
$E_1$	$E_1$
$E_2$	$-I_1 R_{L1}$
$E_{g1}$	$E_1 - E_K$
$E_d$	$E_{bb}$

It can be shown that the circuit cannot remain for an infinite time in this state since the only d-c connection to the grid of  $T_2$  is through the resistance to the cathode of  $T_1$ . If allowed to do so,  $E_2$  would asymptotically approach a final value of  $E_K$  but is restrained from doing this since  $T_2$  will begin to conduct current when the grid voltage reaches the cut-off voltage  $E_{co2}$ . At this time, the circuit will regenerate to its original stable state.

The voltage, as a function of time, at the grid of  $T_2$  during this period can be given by the equation:

$$E_2 = E_f - (E_f - E_i) e^{-\frac{t}{\tau}} \quad 3.7$$

where

$$E_f = E_K = E + I_1 R_K \quad 3.8$$

and

$$E_i = - I_1 R_{L1} \quad 3.9$$

The time constant  $\tau$  is defined as the product of the capacitance and the effective resistance through which the capacitor charges. This time constant will be determined once the region of operation; i.e., saturation or active, of  $T_1$  is known.

By the substitution of  $E_{co2}$  for  $E_2$  in Eq. 3.7, the solution for the period of time  $T$  spent in the quasi-stable state yields:

$$T = \tau \ln \left[ \frac{E + I_1 R_K + I_1 R_{L1}}{E + I_1 R_K - E_{co2}} \right] \quad 3.10$$

where

$$E_{co2} = - \frac{E_{bb}}{\mu} \quad 3.11$$

The idealized voltage waveforms, as determined from the data given in Tables I and II, are given in Fig. 3.4, where the divergence from the calculated values is shown by the dotted lines. The grid of

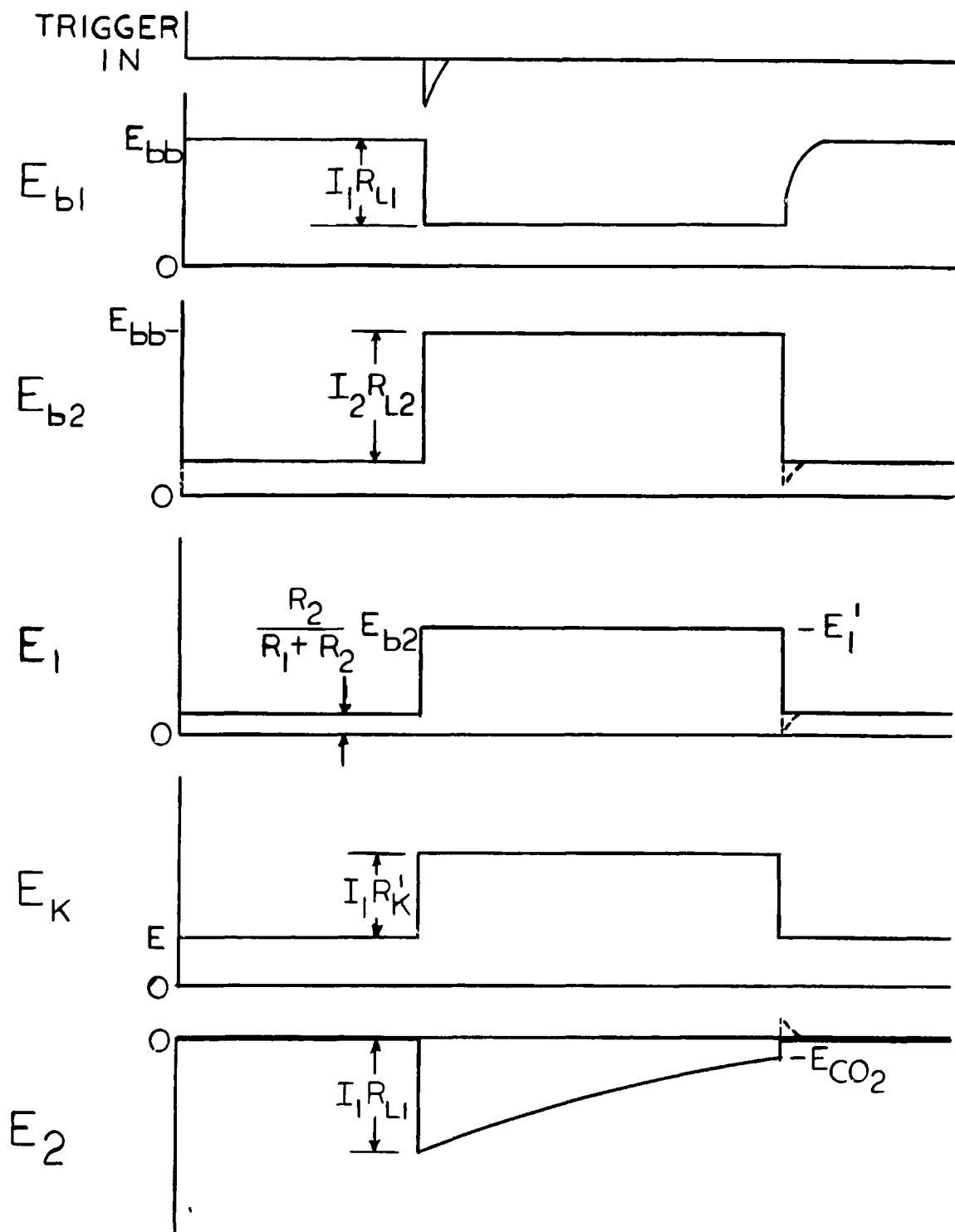


FIGURE 3.4

IDEALIZED VOLTAGE WAVEFORMS OF THE  
VACUUM-TUBE MONOSTABLE MULTIVIBRATOR

$T_2$  is actually driven slightly positive and accounts for the various overshoots. Since the overshoots are small and the time needed for the voltages to decay to their final value is short, in comparison to  $T$ , the net effect on the operation of the circuit is negligible and will be omitted from the analysis to follow.

### 3.4 CALCULATION OF THE TIMING PERIOD

A value must be determined for  $I_1$  and  $\tau$  in order to express Eq. 3.10 as a function of the circuit parameters. A load line must be plotted on the plate characteristic curves of  $T_1$ . In order to plot the load line, it is necessary to find the value of the effective plate voltage and load resistance that comprise the external circuit of  $T_1$ . The resultant circuit is shown in Fig. 3.5 where

$$R_t \cong R_{L1} + R_K \quad 3.12$$

$$E_t \cong E_{bb} - E \quad 3.13$$

since

$$R \gg R_{L1} + R_K \quad 3.14$$

From these equations, the appropriate load line can be constructed.

The value of  $e_{g1}$  which locates the operating point of the tube is given by the equation

$$e_{g1} = E_1 - E - I_1 R_K \leq 0 \quad 3.15$$

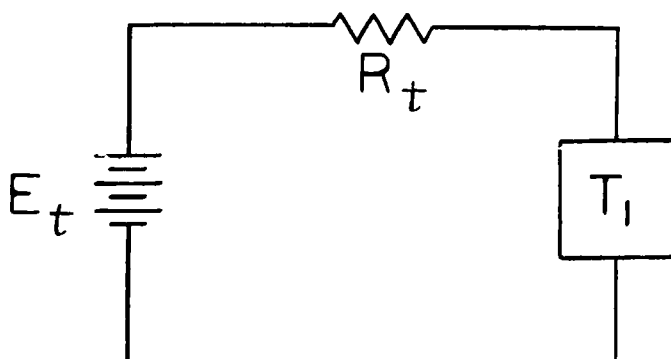


FIGURE 3.5

EFFECTIVE PLATE SUPPLY VOLTAGE AND LOAD  
RESISTANCE OF TUBE  $T_1$  FOR OPERATION IN REGION II

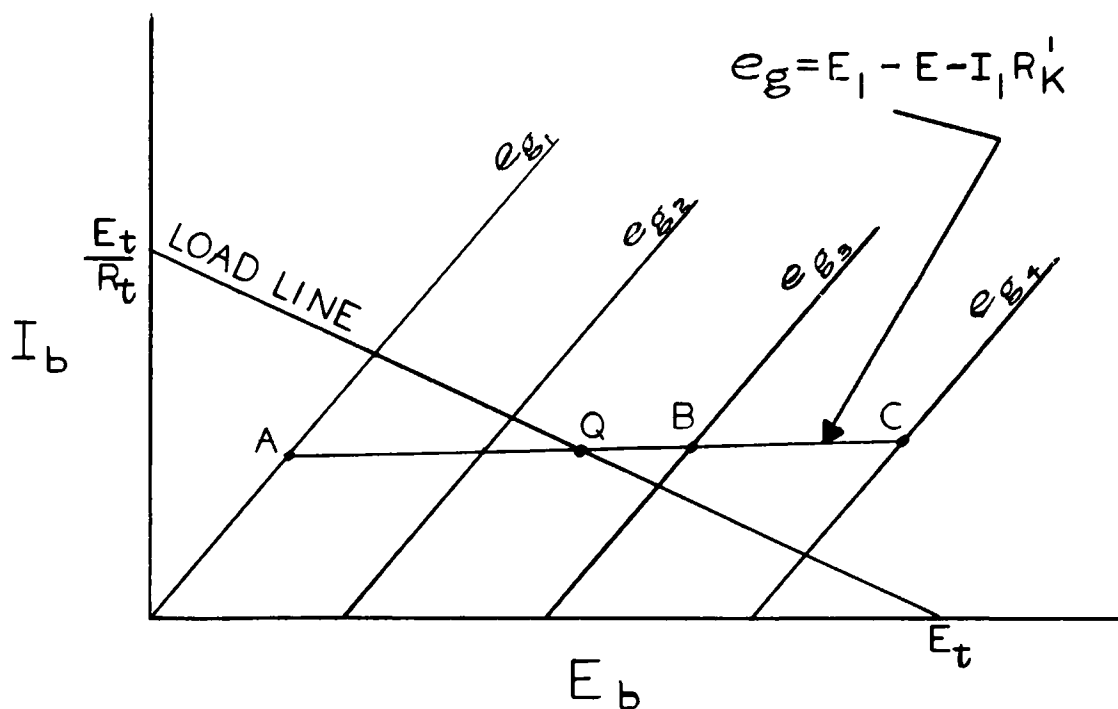


FIGURE 3.6

GRAPHICAL METHOD FOR DETERMINING THE OPERATING  
POINT OF  $T_1$  FOR OPERATION IN THE QUASI-STABLE STATE

The actual value for this voltage will be negative or zero but never positive due to the clamping action previously discussed. If Eq. 3.15 should yield a positive number it only indicates that the grid is clamped to the cathode voltage.

Since there are two variables present in the above equation, a trial and error solution is necessary. A graphical method is described by Millman and Taub<sup>2</sup> where values are assumed for  $I_1$  with  $e_{g1}$  calculated from the equation. These values determine a curve which is also plotted on the plate characteristic curves. The intersection of this curve with the load line determines the operating point of the tube. This method is depicted in Fig. 3.6. It is possible that the operating point could fall to the left of the  $e_{g1} = 0$  curve which would emphasize the fact that  $T_1$  is in clamp.

Replacing the tubes with their appropriate circuit models yields the circuit shown in Fig. 3.7 where the switch is closed, and  $T_1$  is in a clamped condition. The current  $I_1$ , as determined from this circuit when the current through  $R$  is assumed to be negligible, is given by the equations:

$$I_1 \text{ clamp} = \frac{E_{bb} - E}{R_{L1} + r_p + R_K} \quad 3.16$$

$$I_1 \text{ active} = \frac{E_{bb} + \mu_1 E_1 - E(\mu_1 + 1)}{r_p + R_{L1} + R_K(\mu_1 + 1)} \quad 3.17$$

<sup>2</sup>J. Millman and H. Taub, Pulse and Digital Circuits, McGraw-Hill Book Co., Inc., 1956, pp. 13-15

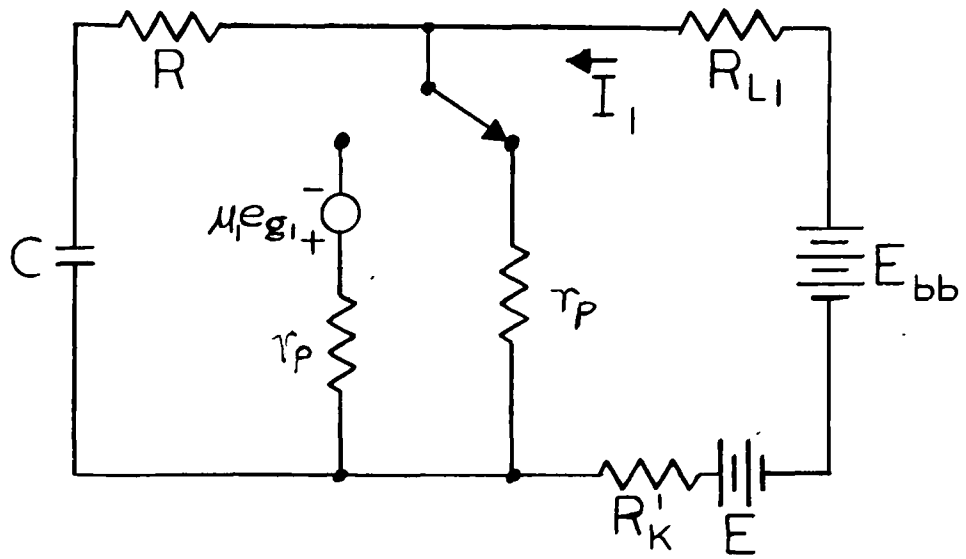


FIGURE 3.7

SIMPLIFIED EQUIVALENT CIRCUIT FOR  
OPERATION IN THE QUASI-STABLE STATE

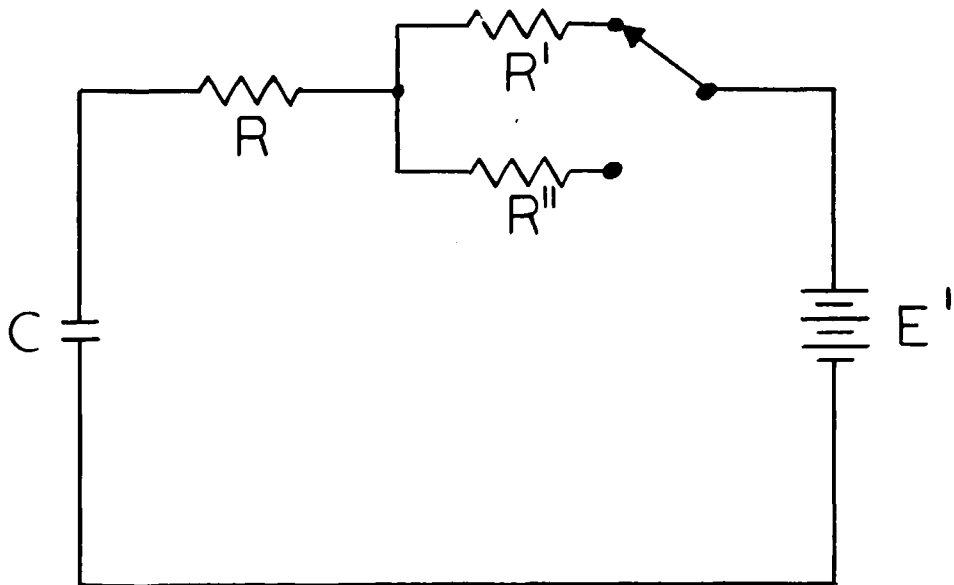


FIGURE 3.8

CALCULATION OF THE TIME CONSTANT FOR  
OPERATION IN THE QUASI-STABLE STATE

where the values for  $r_p$  and  $\mu_1$  are determined graphically at the point of operation of  $T_1$ .

By simplifying the circuit in Fig. 3.7 to that of Fig. 3.8, we can determine the time constant  $\tau$ , which has a value of:

$$\tau_{\text{clamp}} = (R'' + R) C \cong RC \quad 3.18$$

$$\tau_{\text{active}} = (R'' + R) C \quad 3.19$$

where the assumptions

$$R'' \cong r_p \quad R \gg R''$$

$$R'' \cong R_{L1} + R_{K'} \quad r_p < R_{L1} + R_{K'}$$

have been made.

Equations 3.16 through 3.19 make it possible to express Eq. 3.10 in terms of the circuit parameters, and after simplification has values given by the equations:\*

$$\tau_{\text{clamp}} = (R) (C) \ln \left[ \frac{R_K(r_p + R_{L1} + R_3) + R_{L1} R_3}{R_K(r_p + R_{L1} + R_3) + R_3 \frac{R_{L1}}{\mu_2}} \right] \quad 3.20$$

$$\tau_{\text{active}} = (R'' + R) C \ln \left\{ \frac{R_K R_{L1} [r_p + R_{L1} (1 - \mu_1) + R_3] + R_K R_2 R_3 (\mu_1 + 1) + R_2 R_3 R_{L1} (\mu_1 + 1)}{R_K R_{L1} [r_p + R_{L1} + R_3 (1 + \frac{\mu_1}{\mu_2})] + R_K R_2 R_3 (\mu_1 + 1 + \frac{\mu_1}{\mu_2})} \right\} \quad 3.21$$

The plate supply voltage does not appear in these equations and illustrates the independence of the timing period of  $E_{bb}$ . However, the values for  $r_p$ ,  $\mu_1$ , and  $\mu_2$  depend to some extent on  $E_{bb}$  but will

---

\*See Appendix A

cause only a slight variation in  $T$  for moderate changes about the design value of  $E_{bb}$ . In Chapter 5, measurements will be made to determine the percentage change in  $T$  for various changes in the supply voltage.

### 3.5 TRIGGERING OF THE MONOSTABLE MULTIVIBRATOR

Upon the termination of the quasi-stable state, the circuit reverts to its stable mode of operation and remains there until another trigger pulse is applied. If the method to be discussed below is employed, the circuit will not respond to the incoming trigger until  $E_{b1}$  has reached its final value of voltage. The recovery time of  $E_{b1}$  then limits the rate at which the triggers may be applied.

Let us refer to Fig. 3.2 to obtain the value for the time constant that dictates the recovery of  $E_{b1}$ . The time constant  $\tau_1$  has a value given by the equation:

$$\tau_1 = (R_{L1} + r_g) C \cong R_{L1} C \quad 3.22$$

where it has been assumed that  $R_{L1}$  is much larger than  $r_g$ . Fig. 3.9 shows an example of a decaying exponential waveform plotted with the percentage of voltage remaining versus the number of time constants that have elapsed. A trigger pulse which is applied prematurely to the circuit, before  $E_{b1}$  fully recovers, could cause the timing period to be foreshortened. In order to prevent this, it is necessary to allow  $E_{b1}$  to essentially reach its final value of voltage. As may be observed from the exponential waveform of Fig. 3.9, it takes an infinite number of time constants to reach the final value of voltage. For the

accuracies involved in this thesis, it will be adequate to allow approximately five time constants to elapse before the application of the trigger. The maximum rate at which the trigger pulses should be applied is then defined by the equation:

$$T \text{ (Trigger)} = T + 5\tau_1 \quad 3.23$$

The method and type of triggering are also important and there are a number of different ways in which triggering may be accomplished. One method of triggering is by the application of a positive pulse to the normally off grid of  $T_1$ ; however, this requires a very large pulse in most instances because of the large negative bias necessary to insure that  $T_1$  is held cut off. For the circuit under discussion, a positive pulse of amplitude

$$E_T > E_1 - E + E_{col} \quad 3.24$$

would be required. It is also quite possible that the negative-going portion of the positive triggering pulse will cause a reverse transition and destroy the action of the multivibrator. This is often the case since it requires a much smaller pulse to drive the tube back into cut off than was necessary to place the tube into operation. A negative trigger, therefore, is much more effective than a positive one.<sup>3</sup>

A preferable method of triggering then, is the application of a negative pulse to the grid of  $T_2$  or to the plate of  $T_1$  which is

---

<sup>3</sup>J. Millman and H. Taub, Pulse and Digital Circuits, McGraw-Hill Book Co., Inc., 1956, pp. 156-159

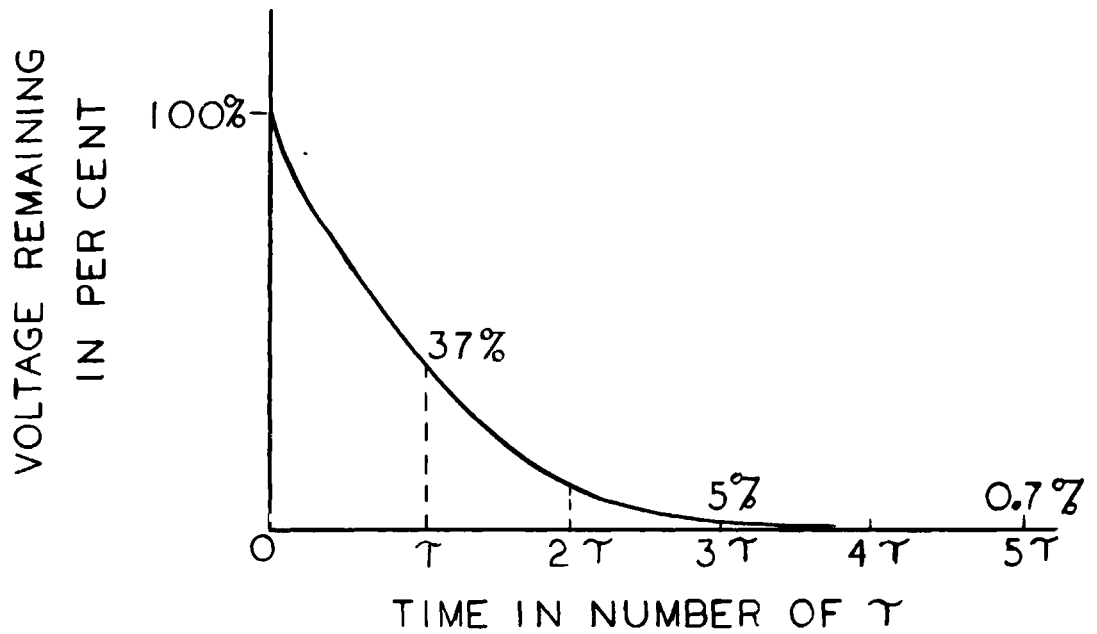


FIGURE 3.9

GENERALIZED EXPONENTIAL WAVEFORM

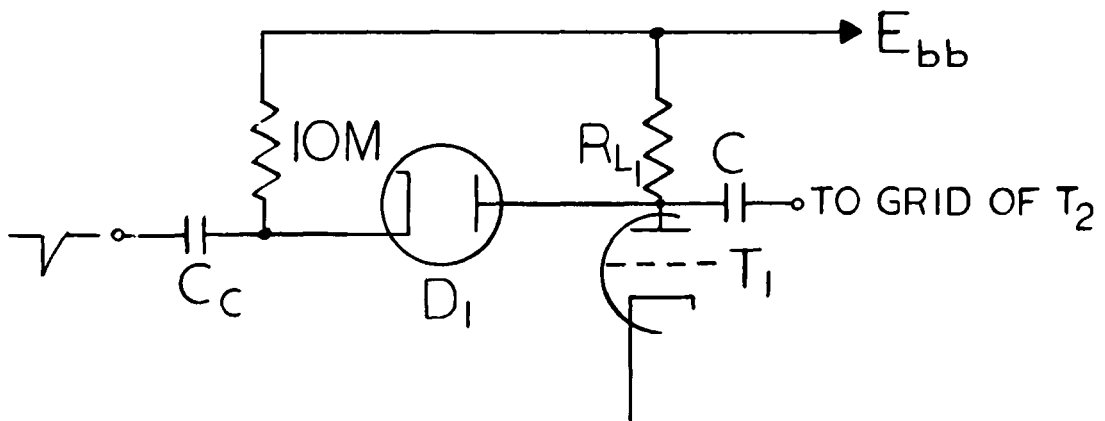


FIGURE 3.10

RECOMMENDED METHOD FOR TRIGGERING THE  
VACUUM-TUBE MONOSTABLE MULTIVIBRATOR

coupled to the grid of  $T_2$  by the capacitor C. This triggering arrangement is illustrated in Fig. 3.10. At the instant of the transition, the plate of  $T_1$  will drop in voltage and reverse bias the diode causing the triggering signal to be decoupled from the multivibrator until the completion of the quasi-stable state. This results in a much more reliable action.

The method of triggering may be dictated by considerations other than those mentioned, however the importance of the subject is not intended to be deemphasized since proper circuit action is dependent upon reliable triggering.

## CHAPTER 4

### ANALYSIS OF THE TRANSISTOR MONOSTABLE MULTIVIBRATOR

#### 4.1 INTRODUCTION

Transistors have numerous advantages over vacuum tubes, in particular: they are much smaller in size, they require no filament power, they operate at a lower supply voltage, they have lower power dissipation, and they normally have a longer operating life than tubes. The superior switching properties of transistors, as may be observed from the circuit models of Chapter 2, make them particularly well suited for application in switching circuits.

The circuit of Fig. 4.1 is the transistor counterpart of the vacuum tube circuit considered previously. The voltages and currents are defined as shown in Figure 4.1.

#### 4.2 STABLE STATE OPERATION

By the proper selection of  $R_2$  and  $R_E$ , the operation of transistor  $T_1$  is designed to be held in the cut-off condition and transistor  $T_2$  to be in clamp. This condition is necessary to assure reliable operation of the circuit and to take advantage of the excellent switching properties of the transistors. For this condition, the circuit can be reduced to the circuit given in Fig. 4.2 where the transistors have been replaced by their circuit models and the values

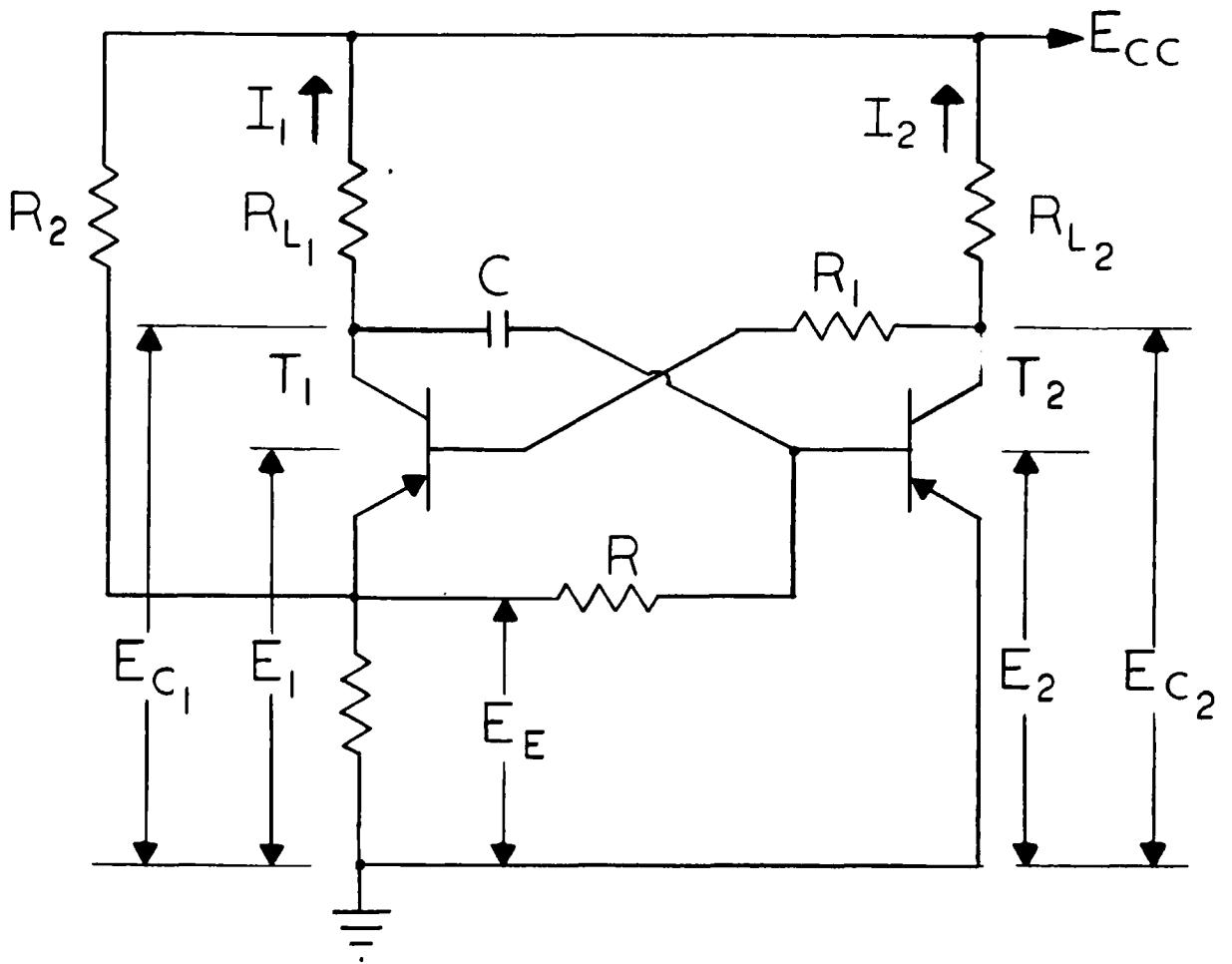


FIGURE 4.1

TRANSISTOR MONOSTABLE MULTIVIBRATOR

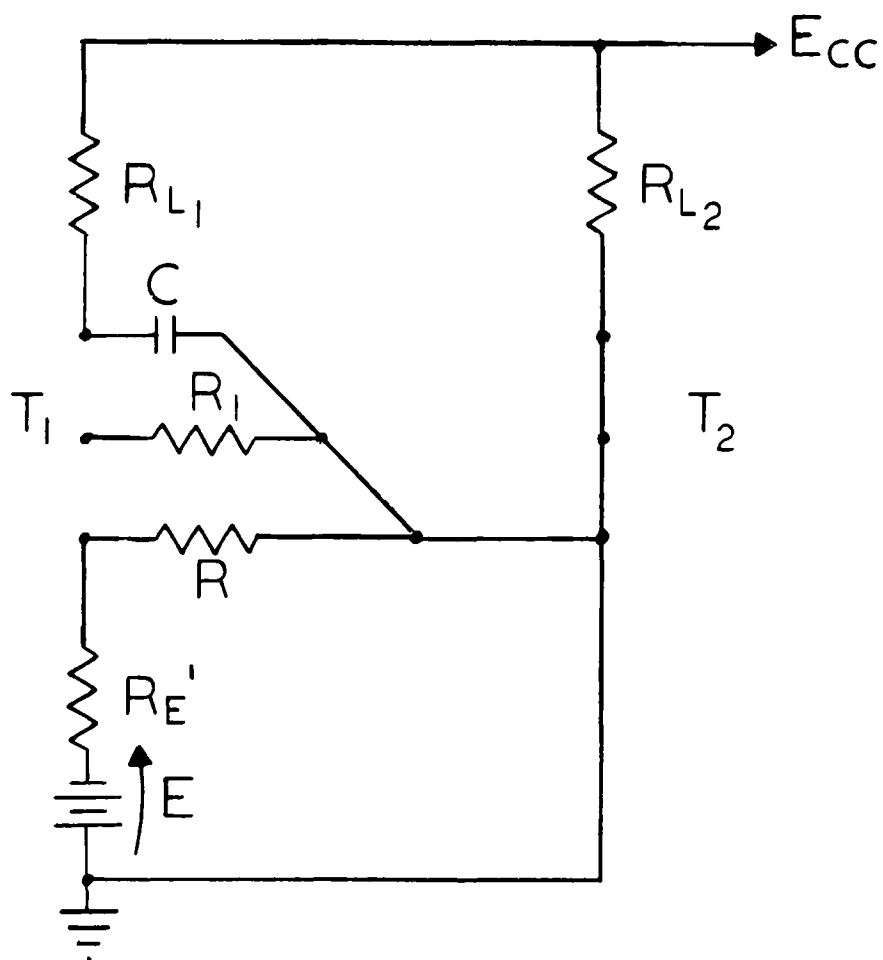


FIGURE 4.2

EQUIVALENT CIRCUIT FOR OPERATION IN THE STABLE STATE

for  $R_E'$  and  $E$  are given by the equations:

$$R_E' = \frac{R_E R_2}{R_E + R_2} \quad 4.1$$

$$E = \frac{E_{CC} R_E}{R_E + R_2} \quad 4.2$$

A selection for the value of either  $R_2$  or  $R_E$  is initially made with the other to be calculated after the desired magnitude for  $E$  has been established.

The base current necessary to drive  $T_2$  into saturation specifies that  $E$  have a magnitude of:

$$E > I_{B0} R \quad 4.3$$

where  $I_{B0}$  is defined by the intersection of the load line with the line created by the merging of the current curves as shown in Fig. 2.7(a). The requirement that  $T_1$  be cut off is also satisfied by the value of  $E$  as given in Eq. 4.3.

The voltages that result from operation in this state are given in Table III where

$$R \gg R_E' \quad 4.4$$

TABLE III

## TRANSISTOR STABLE STATE VOLTAGE EQUATIONS

VOLTAGE	VALUE
$E_{c1}$	$E_{cc}$
$E_{c2}$	$\cong 0$
$E_1$	$\cong 0$
$E_2$	$\cong 0$
$E_E$	$E$

These conditions, specified by Table III, will prevail until the application of an external trigger causes a transition to the quasi-stable state.

## 4.3 QUASI-STABLE STATE OPERATION

Upon the application of a trigger pulse, transistor  $T_2$  is cut off and  $E_{c2}$  drops quickly to  $E_{cc}$ ; this, in turn, causes  $T_1$  to be driven into saturation through its base connection to the collector of  $T_2$ . At this instant of time, the equivalent circuit is given by Fig. 4.3 where the transistors have again been replaced by their circuit models. The voltages are calculated from this circuit and have the values given in Table IV.

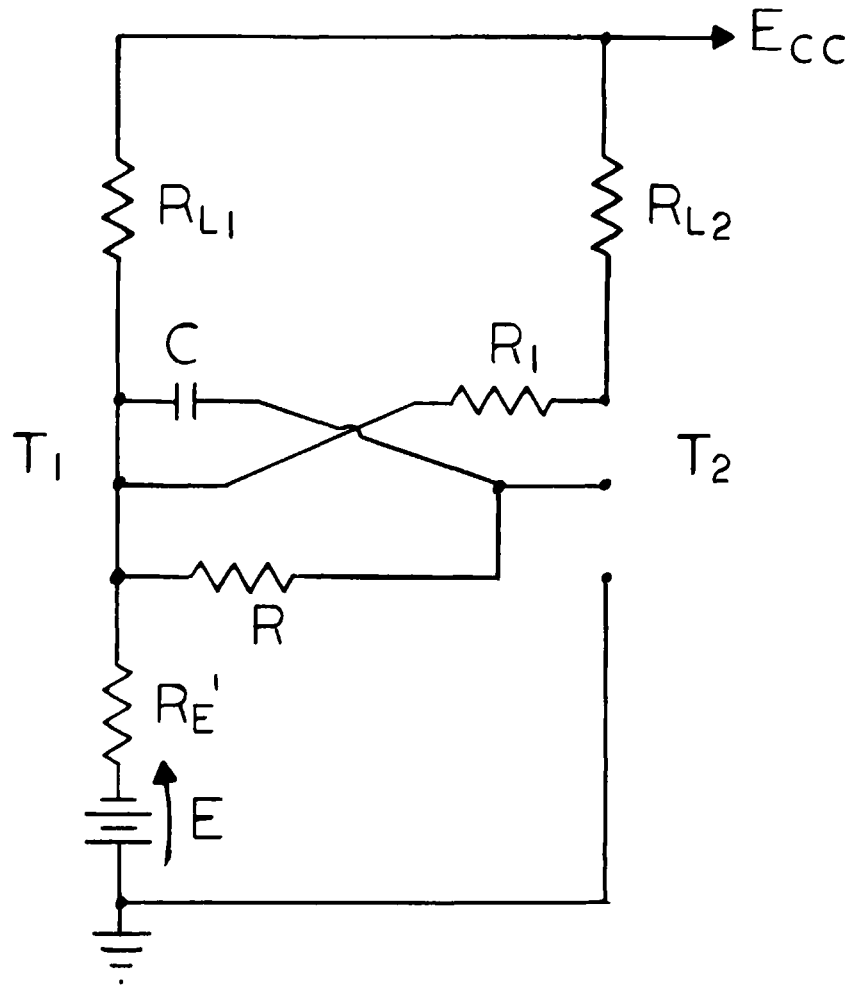


FIGURE 4.3

EQUIVALENT CIRCUIT FOR OPERATION IN THE QUASI-STABLE STATE

TABLE IV

## TRANSISTOR QUASI-STABLE STATE VOLTAGE EQUATIONS

VOLTAGE	VALUE
$E_{c1}$	$E_{cc} + I_1 R_{L1}$
$E_{c2}$	$E_{cc}$
$E_1$	$E_E$
$E_2$	$I_1 R_{L1}$
$E_E$	$E - I_1 R_E$

The current  $I_1$  and time constant  $\tau$  are also calculated from Fig. 4.3 and have values represented by:

$$I_1 = \frac{-E_{cc} + E}{R_{L1} + R_E} \quad 4.5$$

$$\tau = RC \quad 4.6$$

where it is assumed that

$$\frac{R_E}{R_E + R_{L2} + R_1} \ll 1 \quad 4.7$$

If allowed to do so, the voltage at the base of  $T_2$  would asymptotically approach a final value of  $E_E$ . The voltage  $E_2$  is restrained from doing this, however, by the conduction of  $T_2$  when the voltage reaches a value of zero which causes regeneration to the stable state.

The voltage  $E_2$  then changes according to Eq. 3.5 where

$$E_f = E - I_1 R_E \quad 4.8$$

$$E_i = I_1 R_{L1} \quad 4.9$$

Solution of Eq. 3.5 for the period  $T$  will yield a value given by the equation:

$$T = \tau \ln \left[ \frac{E - I_1 R_E - I_1 R_{L1}}{E - I_1 R_E} \right] \quad 4.10$$

which; by the substitution of Eqs. 4.1, 4.2, 4.5, and 4.6, simplifies to the following equation:\*

$$T = RC \ln \left[ 1 + \frac{R_2 R_{L1}}{R_E (R_{L1} + R_2)} \right] \quad 4.11$$

One cycle of operation has now been completed and the idealized voltage waveforms, specified by the data of Tables III and IV, are shown in Fig. 4.4. The entire operation will be repeated upon the application of another trigger pulse.

#### 4.4 TRANSISTOR CIRCUIT TRIGGERING

The method of triggering this circuit is analogous to that employed for the vacuum tube circuit and will not be discussed further in this Chapter. The only difference is one of voltage polarity and magnitude and not one of method. The maximum rate of triggering is

---

\*See Appendix B

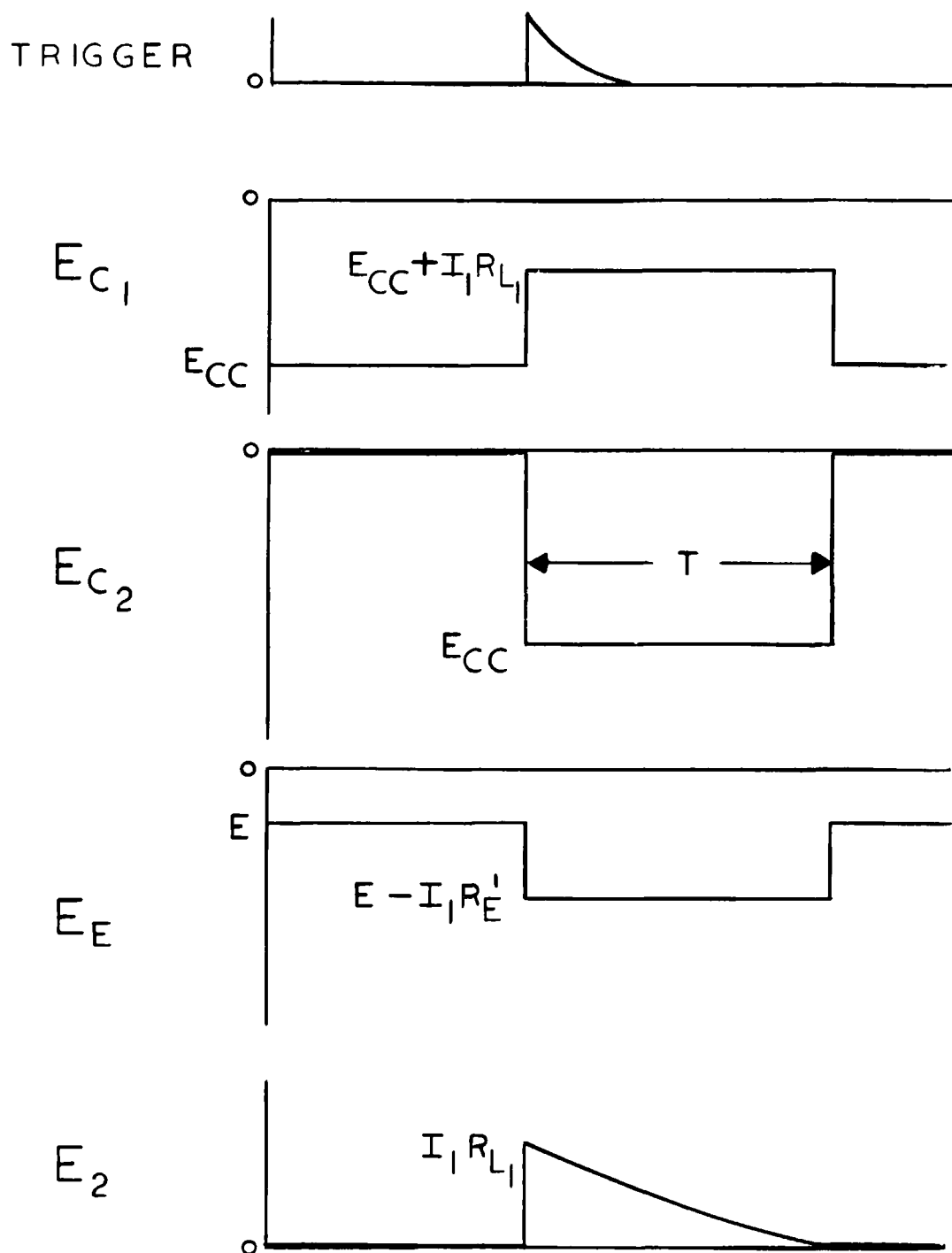


FIGURE 4.4

IDEALIZED VOLTAGE WAVEFORMS OF  
THE TRANSISTOR MONOSTABLE MULTIVIBRATOR

again limited by the decay of  $E_{C1}$  to its final value. This is defined by Eq. 3.23 where  $\tau_1$  for this circuit is calculated from Fig. 4.2 and is given by:

$$\tau_1 = (R_{L1}) (C) \quad 4.12$$

This completes the analysis of the transistor circuit.

## CHAPTER 5

### EXPERIMENTAL TEST RESULTS

#### 5.1 TEST PROCEDURE

In order to substantiate the validity of the mathematical analysis, experimental circuits were constructed and tested for both the vacuum-tube and transistor circuits. Figure 5.1 shows a block diagram of the experimental setup used to obtain the various measurements. The measured values will be compared with the values calculated from the mathematical formulas of Chapters 3 and 4. The vacuum-tube circuit is considered first.

#### 5.2 VACUUM-TUBE EXPERIMENTAL RESULTS

Since the equation for the timing period of the unclamped case is much more complex and more dependent upon the tube parameters, it is anticipated that more reliable and satisfactory results are obtained from the clamped case. It is felt, however, that the unclamped case would exhibit excellent independence of changes in the supply voltage, but would be very sensitive to other factors, such as tube replacements, tube aging, and filament voltage change. Since preliminary tests verified these assumptions, the author highly recommends the circuit where  $T_1$  is in clamp during the quasi-stable state. A circuit of this configuration was designed and is shown in Fig. 5.2.

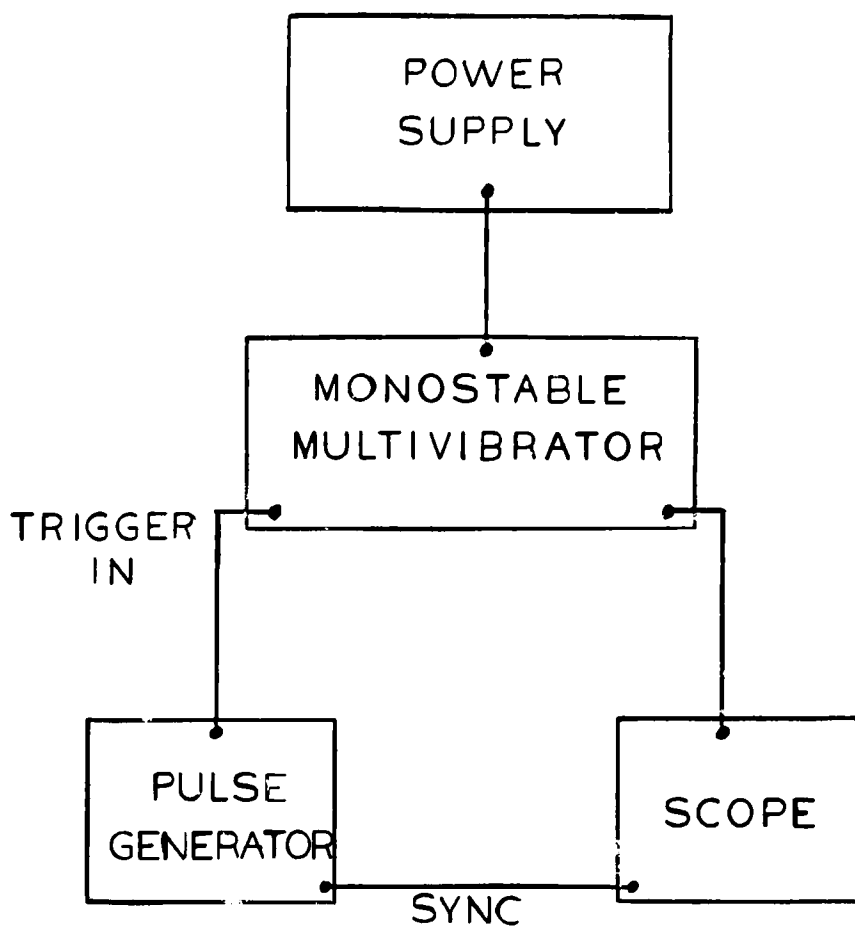


FIGURE 5.1

BLOCK DIAGRAM OF THE EXPERIMENTAL SETUP

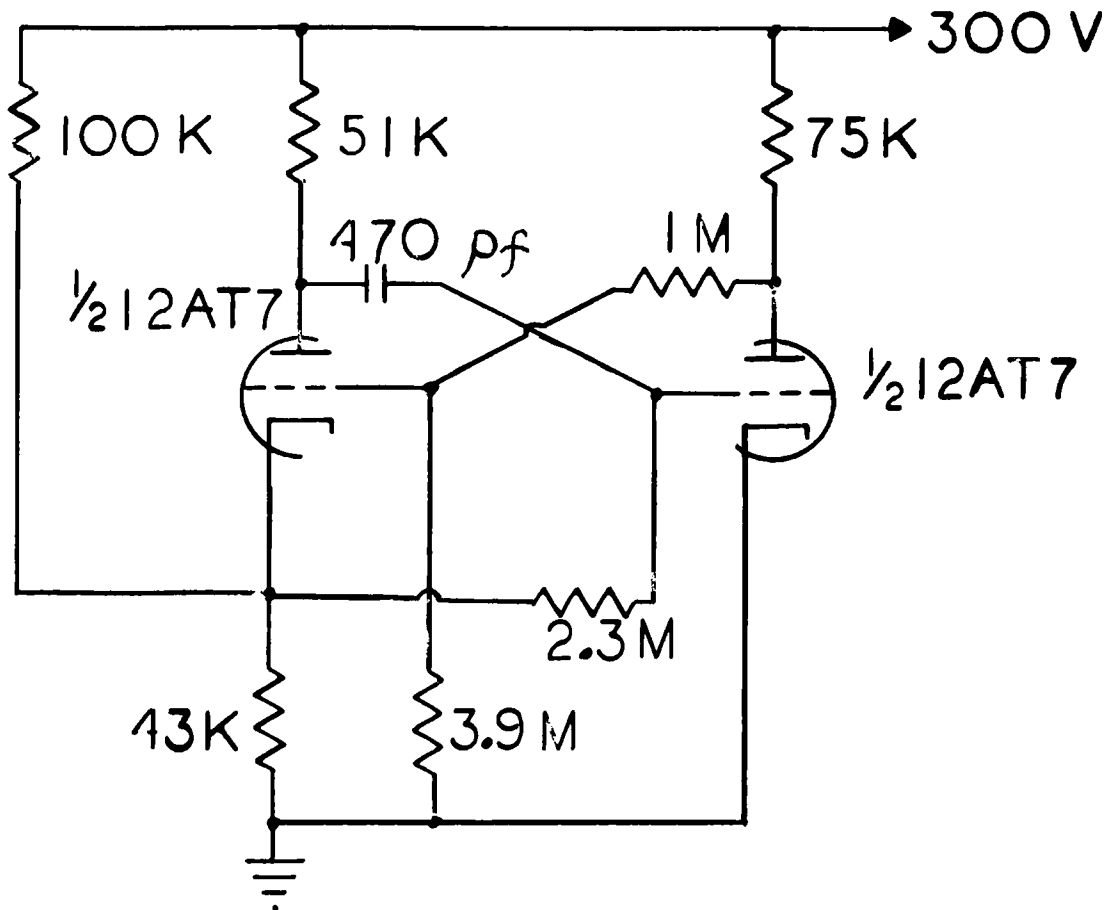


FIGURE 5.2

EXPERIMENTAL VACUUM-TUBE MONOSTABLE MULTIVIBRATOR

The indicated circuit parameters were selected for the following reasons:  $R_{L2}$  to provide an output swing of approximately 200 volts,  $R_3$  and  $R_K$  to satisfy Eqs. 3.1 and 3.4,  $R_1$  and  $R_2$  to hold  $T_1$  in clamp during the quasi-stable state,  $R$  and  $C$  to give a timing period of 500 microseconds, and  $R_{L1}$  to cause the argument of the logarithm of Eq. 3.20 to have as large a value as possible. The argument of the logarithm must be kept large in order to minimize the effect that small changes in  $r_p$  and  $\mu_2$  will have on the value of the timing period. The resistor  $R_{L1}$  is selected to satisfy this requirement since the remaining components are specified by other considerations. This resistor cannot have too large a value, however, and a compromise must be made.

The load lines, corresponding to the above components, are plotted on the plate characteristic curves of the 12AT7, a twin-triode frequently used as an oscillator, and appear as shown in Fig. 5.3. The values for  $r_p$  and  $\mu_2$  are found graphically from these curves and have values of 30 kilohms and 25 respectively. Since it is verified, both mathematically and experimentally, that  $T_1$  is in clamp during the quasi-stable state, the above values may be utilized to solve Eq. 3.20 for the resistance  $R$  and capacitance  $C$ . For the given value of 470 picofarads for  $C$ , a value of 2.3 megohms for  $R$  is necessary in order to have a timing period duration of 500 microseconds. It is normal practice for the components to be 10% units whenever possible, and this practice is followed here with the exception of  $R$  and  $C$  which are 1% precision units. This choice allows a more realistic

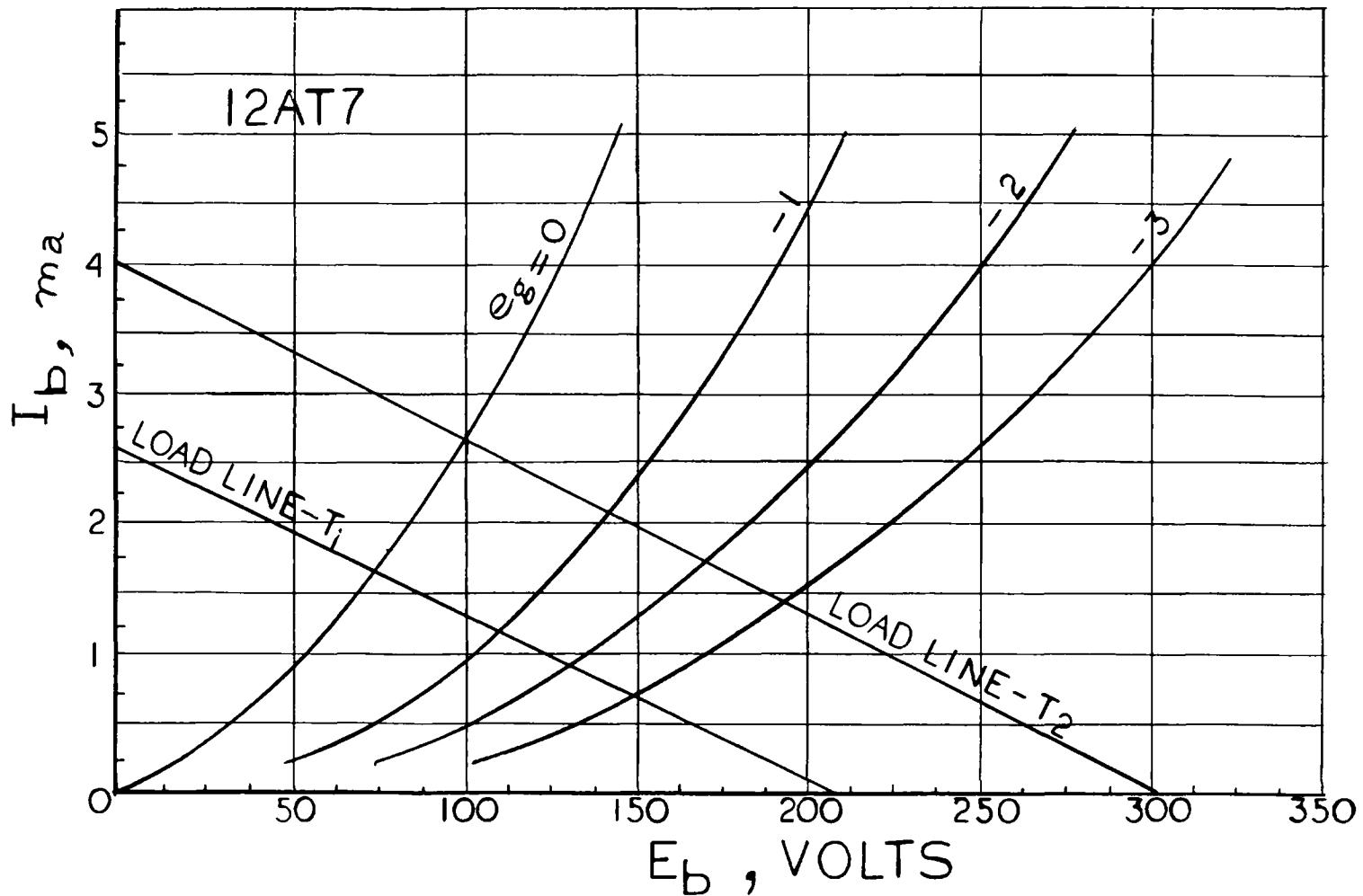


FIGURE 5.3  
CHARACTERISTIC CURVES FOR A 12AT7  
VACUUM-TUBE TRIODE

comparison to be made between the calculated and measured results.

Table V gives the calculated versus measured values of voltage for both the stable state and the quasi-stable state.

TABLE V  
EXPERIMENTAL RESULTS FOR THE VACUUM-TUBE  
MONOSTABLE MULTIVIBRATOR CIRCUIT

MEASURED AND CALCULATED VOLTAGE VALUES

VOLTAGE	STABLE	STATE	QUASI-STABLE STATE	
	CALCULATED	MEASURED	CALCULATED	MEASURED
$E_{b1}$	300	300	216	200
$E_{b2}$	100	90	300	290
$E_1$	79	60	140	160
$E_2$	0	0	-84 to 0	-100 to 0
$E_K$	90	90	140	160

The measured value for  $T$  is 485 microseconds and compares favorably with the design value of 500 microseconds, an error of only three per cent. A measurement was made to determine the sensitivity of the timing period to changes in the supply voltage. The waveforms of Fig. 5.4 indicate the change in  $T$  when  $E_{bb}$  is varied in 50 volt increments from 300 volts to 150 volts. The lower set of waveforms in Fig. 5.4 shows the expanded trailing edge of  $E_{b2}$ , which allows an accurate measurement to be made when  $E_{bb}$  is varied in the above manner. These results are summarized in Table VI where

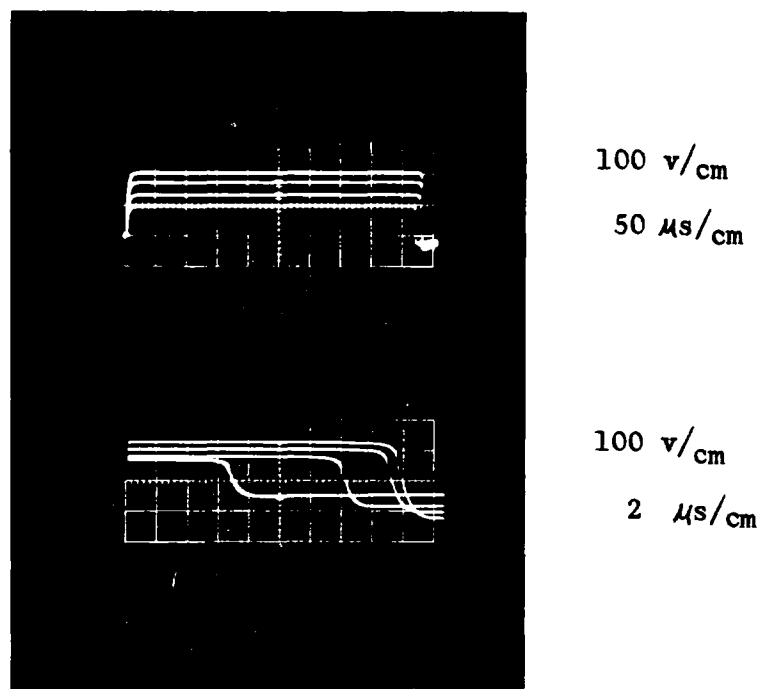


FIGURE 5.4

OUTPUT WAVEFORM OF THE VACUUM-TUBE MONOSTABLE  
MULTIVIBRATOR FOR DIFFERENT VALUES OF SUPPLY VOLTAGE

$$\% \text{ change in } E_{bb} = \frac{300 - E_{bb}}{300} \times 100 \% \quad 5.1$$

$$\% \text{ change in } T = \frac{T_{300} - T}{T_{300}} \times 100 \% \quad 5.2$$

TABLE VI

EXPERIMENTAL RESULTS FOR THE VACUUM-TUBE MONOSTABLE  
MULTIVIBRATOR CIRCUIT

PER CENT CHANGE IN T VERSUS PER CENT CHANGE IN  $E_{bb}$

$E_{bb}$	% Change in $E_{bb}$	T	% Change in T
300	0	485	0
250	16.7	485	0
200	33.3	481	0.83
150	50	474	2.3

### 5.3 TRANSISTOR EXPERIMENTAL RESULTS

The values of the circuit parameters shown in Fig. 5.5 were selected for the following reasons:  $R_{L2}$  to limit the current that flows through the collector of  $T_2$ ,  $R_2$  and  $R_E$  to satisfy Eqs. 4.2 and 4.3,  $R_1$  to limit the base current of  $T_1$  when it is in clamp, R and C to provide a timing period of 50 microseconds, and  $R_{L1}$  to cause the argument of the logarithm of Eq. 4.11 to have as large a value as possible. It is again necessary to make a compromise as the value of  $R_{L1}$  should not become excessive.

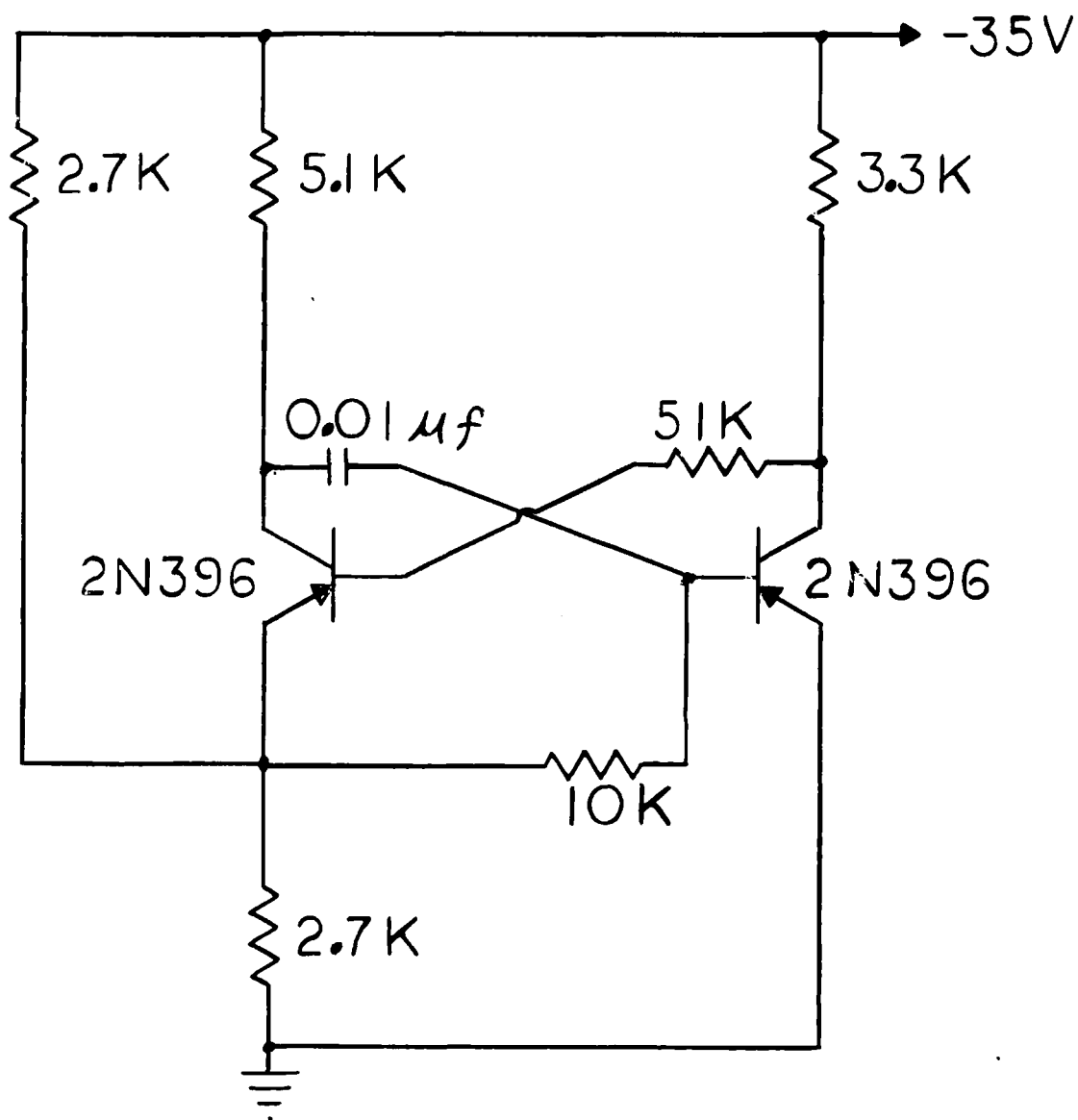


FIGURE 5.5

EXPERIMENTAL TRANSISTOR MONOSTABLE MULTIVIBRATOR

Two p-n-p switching transistors, 2N396's, were utilized in the experimental circuit. For a given value of 0.01 microfarads for C, a value of 10 kilohms for R is necessary in order to have a timing period of 50 microseconds. In order to make a more realistic comparison between the calculated and measured values, precision units were again selected for R and C. Table VII shows the calculated versus measured values of voltage for both the stable state and quasi-stable state. The measured value for T is 49 microseconds and indicates excellent correlation with the calculated value of 50 microseconds.

TABLE VII

EXPERIMENTAL RESULTS FOR THE TRANSISTOR MONOSTABLE  
MULTIVIBRATOR CIRCUIT

MEASURED AND CALCULATED VOLTAGE VALUES

VOLTAGE	STABLE STATE CALCULATED	STABLE STATE MEASURED	QUASI-STABLE CALCULATED	QUASI-STABLE MEASURED
$E_{c1}$	-35	-35	-21	-21
$E_{c2}$	0	0	-35	-32
$E_1$	0	0	-21	-22
$E_2$	0	0	14 to 0	14 to 0
$E_E$	-17.5	-16	-21	-22

The waveforms of Fig. 5.6 indicate the change in T when  $E_{cc}$  is varied from -35 volts to -17.5 volts. The lower set of waveforms shows the trailing edge of  $E_{c2}$  which gives a very accurate indication

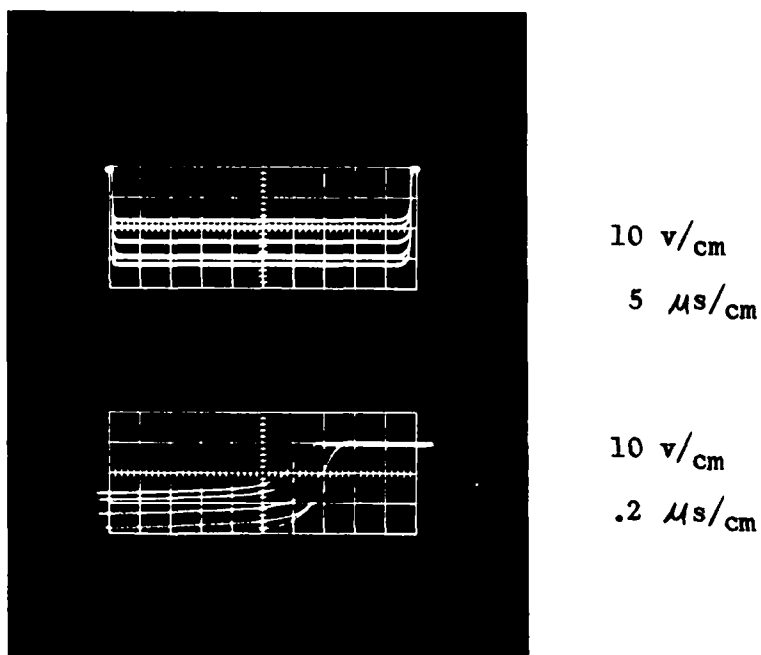


FIGURE 5.6

OUTPUT WAVEFORM OF THE TRANSISTOR MONOSTABLE  
MULTIVIBRATOR FOR DIFFERENT VALUES OF SUPPLY VOLTAGE

of the timing period's independence of the supply voltage. These results are summarized in Table VIII where

$$\% \text{ change in } E_{cc} = \frac{35 - E_{cc}}{35} \times 100\% \quad 5.3$$

$$\% \text{ change in } T = \frac{T_{35} - T}{T_{35}} \times 100\% \quad 5.4$$

TABLE VIII

EXPERIMENTAL RESULTS FOR THE TRANSISTOR MONOSTABLE  
MULTIVIBRATOR CIRCUIT

PER CENT CHANGE IN T VERSUS PER CENT CHANGE IN  $E_{cc}$

$E_{cc}$	% Change In $E_{cc}$	T	% Change in T
-35	0	49.0	0
-30	14.3	49.04	0.08
-25	28.6	49.0	0
-20	42.9	48.9	0.2
-17.5	50	48.75	0.51

## CHAPTER 6

### CONCLUSIONS

#### 6.1 PERFORMANCE EVALUATION

The experimental results of Chapter 5 show excellent correlation with the values calculated from the mathematical formulas of Chapters 3 and 4. The validity of the equations that were developed has been established, and it may also be observed that only negligible errors have occurred due to the approximations that were made. For the specified design conditions, there was only a 3% difference between the measured and calculated values of the timing period. This error can, of course, be made negligible by an adjustment of either R or C.

The desired objective that the timing period be independent of supply voltage has been achieved. A 50% change in the supply voltage resulted in a timing period variation of only 2.3% for the vacuum-tube circuit and 0.51% for the transistor circuit.

#### 6.2 RECOMMENDATIONS FOR FURTHER STUDY

An investigation should be conducted to determine what limits exist on the timing period of these monostable multivibrators. In order to obtain faster waveforms, the rise and fall times of the pulse must be shortened. A study should also be made to determine what effect different trigger pulses would have on these circuits. A possible trouble area, in obtaining longer timing periods, is in

the loading caused by the input resistance of the second stage. This is especially true of the transistor circuit.

The feasibility of obtaining a variable delay from these multivibrators should be investigated. It may be possible to achieve results that are superior to those obtained from the cathode-coupled monostable multivibrator, thus providing a circuit that compares favorably with the phanastron<sup>4</sup> as a stable delay device.

---

<sup>4</sup>J. M. Pettit, Electronic Switching, Timing, and Pulse Circuits, McGraw-Hill Book Company, Inc., New York, 1959, pp 182-187

APPENDIX A

THE DERIVATION OF THE TIMING PERIOD FOR

THE CASE WHERE  $T_1$  IS IN CLAMP

The equation for the timing period of the vacuum-tube monostable multivibrator will be expressed as a function of the circuit parameters. In order to do this, the equations that define  $E$ ,  $I_1$  and  $E_{co2}$  will be substituted into Eq. 3.10 and the ensuing result simplified.

$$T = \tau \ln \frac{E + I_1 R_K' + I_1 R_{L1}}{E + I_1 R_K' - E_{co2}} \quad 3.10$$

where

$$E = \frac{E_{bb} R_K}{R_K + R_3} \quad R_K' = \frac{R_K R_3}{R_K + R_3}$$

$$I_1 (\text{clamp}) = \frac{E_{bb} - \frac{E_{bb} R_K}{R_K + R_3}}{R_{L1} + r_p + \frac{R_K R_3}{R_K + R_3}}$$

$$= \frac{\frac{R_3}{R_{L1} R_K + R_{L1} R_3 + r_p R_K + R_3 r_p + R_K R_3} E_{bb}}{}$$

$$E_{co2} = - \frac{E_{bb}}{\mu_2}$$

Therefore:

$$T = \tau \ln \left\{ \frac{\frac{E_{bb}R_K}{R_K + R_3} + E_{bb} \left\{ \frac{R_K R_3^2 + (R_{L1} R_3)(R_K + R_3)}{[R_{L1}(R_K + R_3) + r_p(R_K + R_3) + R_K R_3]} \right\}}{\frac{E_{bb}R_K}{R_K + R_3} + \left[ \frac{E_{bb}}{R_K + R_3} \right] \left[ \frac{R_K R_3^2}{R_{L1}(R_K + R_3) + r_p(R_K + R_3) + R_K R_3} \right] + \frac{E_{bb}}{\mu_2}} \right\}$$

$$= \tau \ln \left\{ \frac{R_K [R_{L1}(R_K + R_3) + r_p(R_K + R_3) + R_K R_3] + R_K R_3^2 + R_3 R_{L1}(R_K + R_3)}{\left[ \frac{R_K + R_K + R_3}{\mu_2} \right] \left[ R_{L1}(R_K + R_3) + r_p(R_K + R_3) + R_K R_3 \right] + R_K R_3^2} \right\}$$

when

$$\mu_2 \gg 1$$

$$T = \tau \ln \left[ \frac{(R_K + R_3)(R_{L1} R_K + R_K r_p + R_K R_3 + R_{L1} R_3)}{(R_K + R_3)(R_{L1} R_K + R_K r_p + R_K R_3 + \frac{R_3 R_{L1}}{\mu_2} + \frac{R_3 r_p}{\mu_2})} \right]$$

$$= \tau \ln \left[ \frac{R_K (R_{L1} + r_p + R_3) + R_{L1} R_3}{R_K (R_{L1} + r_p + R_3) + \left( \frac{R_3}{\mu_2} \right) (R_{L1} + r_p)} \right] \quad 3.20$$

The derivation for the case where  $T_1$  is operating in the active region is much more involved but follows the same pattern as the above derivation. The simpler case, then, will suffice to illustrate the manner in which the equations for the timing period were derived.

## APPENDIX B

### THE DERIVATION OF THE TIMING PERIOD

#### FOR THE TRANSISTOR CIRCUIT

The equation for the timing period of the transistor monostable multivibrator will be expressed as a function of the circuit parameters. In order to do this, the equations that define  $E$  and  $I_1$  will be substituted in Eq. 4.10 and the ensuing result simplified.

$$\begin{aligned} T &= \tau \ln \left[ \frac{E - I_1 R_{E'} - I_1 R_{L1}}{E - I_1 R_{E'}} \right] = \tau \ln \left[ 1 - \frac{I_1 R_{L1}}{E - I_1 R_{E'}} \right] \\ &= \tau \ln \left[ 1 - \frac{R_{L1}}{\frac{E}{I_1} - R_{E'}} \right] \end{aligned}$$

where

$$\begin{aligned} E &= \frac{E_{CC} R_E}{R_E + R_2} & R_{E'} &= \frac{R_E R_2}{R_E + R_2} \\ I_1 &= \frac{-E_{CC} + E}{R_{L1} + R_{E'}} = -E_{CC} \left[ \frac{-R_E + (R_E + R_2)}{R_{L1}(R_E + R_2) + R_E R_2} \right] \\ &= -E_{CC} \left[ \frac{R_2}{R_{L1}(R_E + R_2) + R_E R_2} \right] \\ \frac{E}{I_1} &= \left[ \frac{E_{CC} R_E}{R_E + R_2} \right] \left[ - \frac{R_{L1}(R_E + R_2) + R_E R_2}{E_{CC} R_2} \right] = - \frac{R_E R_{L1}(R_E + R_2) + R_E^2 R_2}{R_2(R_E + R_2)} \end{aligned}$$

$$T = \tau \ln \left[ 1 + \frac{R_{L1}}{\frac{R_E R_{L1} (R_E + R_2) + R_E^2 R_2 + R_2^2 R_E}{R_2 (R_E + R_2)}} \right]$$

$$T = \tau \ln \left[ 1 + \frac{R_2 R_{L1} (R_E + R_2)}{R_E (R_{L1} + R_2) (R_E + R_2)} \right]$$

$$T = \tau \ln \left[ 1 + \frac{R_2 R_{L1}}{R_E (R_{L1} + R_2)} \right]$$

## BIBLIOGRAPHY

1. Bright, R. L., "Junction Transistors used as Switches", Transactions AIEE, Communications and Electronics, No. 17, pp 111-121, March, 1955.
2. Carroll, J. M., Modern Transistor Circuits, McGraw-Hill Book Company, Inc., New York, 1959.
3. Chance, B., et al., Waveforms, Vol. 19, M.I.T. Radiation Laboratory Series, McGraw-Hill Book Company, Inc., New York, 1949.
4. Hunter, L., Handbook of Semiconductor Electronics, McGraw-Hill Book Company, Inc., New York, 1956.
5. Hurley, R., Transistor Switching Circuits, Sutton Pub. Co., White Plains, New York, 1959.
6. Linville, J. G., "Nonsaturating Pulse Circuits using Two Junction Transistors", Proc. IRE, Vol. 43, pp 826-834, July, 1955.
7. McMahon, R. E., "Designing Transistor Flip-Flops", Electronics Design, Vol. 3, pp 24-27, Oct., 1955.
8. Millman, J. and H. Taub, Pulse and Digital Circuits, McGraw-Hill Book Company, Inc., New York, 1956.
9. Moll, J. L., "Large Signal Transient Response of Junction Transistors", Proc. IRE, Vol. 42, pp. 1773-1778, Dec., 1954.
10. Moskowitz, S. and J. Racker, Pulse Techniques, Prentice-Hall Inc., Englewood Cliffs, New Jersey, 1951.
11. Pettit, J. M., Electronic Switching, Timing, and Pulse Circuits, McGraw-Hill Book Company, Inc., New York, 1959.
12. Ryder, J. D., Electronic Engineering Principles, Prentice-Hall, Inc., Englewood Cliffs, New Jersey, 1956.
13. Sard, E. W., "Junction-Transistor Multivibrators and Flip-Flops", Convention Record of the IRE, 1954 National Convention, Part II, pp 119-124, New York.
14. Shenk, E. R., "The Multivibrator, Applied Theory and Design," Electronics: Part I, Vol. 17, pp 136-141, Jan., 1944; Part II, Vol. 17, pp 140-145, Feb., 1944; Part III, Vol. 17, pp 138-142, March, 1944.